Combining Isothermal and Adiabatic Mode Experiments for Kinetic Constant Estimation: Application to the Hydrogenation of 5-(Hydroxymethyl)furfural (5-HMF)

Sébastien Leveneur

Combining isothermal and adiabatic mode experiments for kinetic constants estimation: application to the hydrogenation of 5-(hydroxymethyl)furfural (5-HMF)

Sebastien Leveneur[1]*

INSA Rouen Normandie, University Rouen Normandie, Normandie Université, LSPC, UR 4704, F-76000 Rouen, France

Email: sebastien.leveneur@insa-rouen.fr

Abstract In the vast majority, kinetic modeling is done in isothermal conditions. The benefit of adiabatic mode is using temperature as an online observable. Nevertheless, in adiabatic mode, one can only get the initial/inlet and final/outlet concentrations, making the development of kinetic models difficult in the presence of several reaction steps. Obtaining kinetic models tested in isothermal and adiabatic modes could change our methodology in kinetic modeling because such models can be used in optimization, thermal risk assessment and pinch analysis. Besides, for chemical systems with several reaction steps, one needs to spend much time to analyze the different samples to get concentration profiles. Thus, developing kinetic models combining isothermal and adiabatic experimental runs could reduce the experimental stage. We tested this methodology in the hydrogenation of 5-(hydroxymethyl)furfural (5-HMF) by using different combinations of adiabatic and isothermal noised synthetic runs. We compared the estimated kinetic constants obtained from these noised synthetic runs with the hypothetical true ones, and the sum of squared residuals. The hypothetical true kinetic constants were created. Global sensitivity analysis using the hypothetical true kinetic constants in isothermal and adiabatic modes was carried out to measure the influence of these constants on the estimated concentration and temperature. We found that implementing some adiabatic runs in a set of experimental runs could be beneficial from a parameter estimation standpoint.

Keywords global sensitivity analysis, Sobol' indices, kinetic modeling, chemical kinetic constants estimation, adiabatic mode, 5-HMF, hydrogenation, Bayesian statistics

1. Introduction

The origin of chemical kinetics started in the 18th and 19th centuries. Several prominent chemists played an essential role, like Lavoisier or Gay-Lussac, who put the basis of chemical observation [1]; Berthollet who made major contributions to the understanding of equilibria phenomena and reaction rates [2]; Berzelius who introduced the concept of catalyst [3] or Arrhenius who showed the relationships between rate constants and temperature [4]. In the 20th century, Hinshelwood worked on developing reaction law and reaction mechanisms [5]. It was vital during this century to predict the concentration, yield, or selectivity in different reactors, i.e., chemical reaction engineering. This science was popularized by famous researchers like Villermaux [6] or Levenspiel [7].

Since then, kinetic modelers have been doing their best to develop kinetic models using experimental and theoretical approaches. These models are fundamental to scaling up a process or optimizing the production process from a yield and energy standpoint.

The development of such models requires prior knowledge about reaction mechanisms to define some rate expression, experimental data that could be noised at different levels, and thermodynamic data such as reaction enthalpy, kinetic of mass transfer, etc.

The obtention and analysis of experimental data are vital to developing reliable kinetic models [8]. Any kinetic modeler knows that the accuracy and complexity of kinetic models depend on the quality of experimental data. Using online measurement to follow kinetics is appealing because one does not interfere with the reaction mixture. Spectroscopy methods like FTIR were used for some cases [9,10] or quadrupole mass spectrometers [11]. Nevertheless, these methods could be limited to the nature of the measured compounds and the nature of the reaction system.

Calorimetry is also an appealing method using temperature or heat-flow rate as a signal [12–18]. Nevertheless, using the calorimetric method requires perfectly characterizing the reactor environment from a thermal viewpoint. For instance, one must verify that the heat loss is negligible, characterize the global heat transfer coefficient value, measure the heat capacity, etc. It is challenging to determine the kinetics of several consecutive or parallel reactions solely based on temperature or heat-flow rate, but not for a single reaction step.

In the case of several reaction steps, the benefits of using a reaction calorimeter in different thermal modes allow us to validate the kinetic models and to get knowledge of heat-flow rate evolution. Such information is essential for pinch analysis or thermal risk assessment.

Zero-order, batch and adiabatic modes are often used for thermal risk assessment because it is the most conservative approach [19]. Experimenting with adiabatic mode also allows us to observe the presence or absence of secondary reactions [20].

Salcedo et al. [21] showed the possibility and the benefits of developing kinetic models in different thermal modes (isothermal, adiabatic and isoperibolic). This approach to developing kinetic models in different thermal modes is rare in the literature [22,23]. Using only a reaction calorimeter to develop a kinetic model for a complex model could be a priori non-sufficient. By complex model, we mean a system with multiphasic and several reactions. To develop kinetic models for such a system, one needs to know the concentration evolution of species [24–26]. Using adiabatic conditions in reaction calorimeters requires no withdrawal of samples to avoid interference with temperature, limiting the kinetic description of all reaction steps. On the other hand, one could imagine combining some experiments in isothermal conditions, including offline analysis, and some in adiabatic conditions, including online reaction temperature. The benefit of adiabatic conditions is that we do not have to analyze several samples during the experiments.

We studied the hydrogenation of 5-(hydroxymethyl)furfural (5-HMF), a multiphasic system with several exothermic reaction steps. Hydrogenation of 5-HMF, issued from the hydrolysis of cellulose, can lead to several interesting molecules used as biofuels or as polymer intermediates [27–36]. This article aimed to determine the impact of the number of adiabatic and isothermal runs on the kinetic modeling. In the first step, we generated synthetic data with different noise levels in isothermal and adiabatic conditions. Using different sets of synthetic runs with noise, we carried out kinetic modeling to determine the kinetic constants and the sum of squared residuals (SSR). It is essential to stress that the hypothetical true kinetic constants used to generate synthetic data were not obtained from laboratory experiments.

2. Generation of synthetic data

This section explains how we generated the synthetic runs without errors, and with the addition of errors to get noised synthetic runs.

2.1 Generation of synthetic data without errors

Figure 1 shows the reaction steps for the hydrogenation of 5-HMF over a virtual catalyst. We imagined that the true mechanism follows a Langmuir-Hinshelwood with the dissociation of hydrogen (LHD1). Hence, the reaction rate for each step can be expressed by Eqs (1)-(3). The inspiration to derive such reaction rates is from the studies of Gyngazova et al., 2017 and Jain and Vaidya, 2016 [32,37].

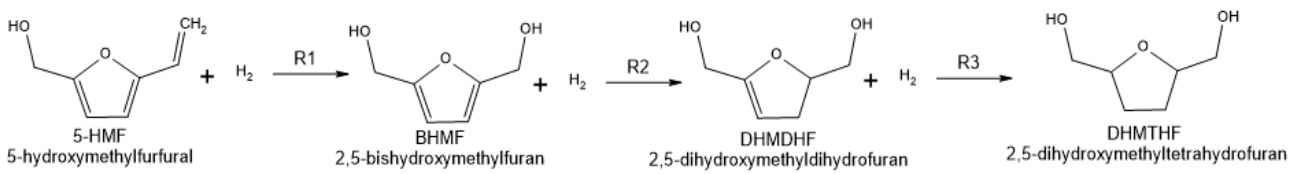

Figure 1. Reaction steps for the hydrogenation of 5-HMF to DHMTHF.

$$R_1 = \frac{k_1 \cdot K_{HMF} \cdot K_H \cdot C_{H2} \cdot C_{HMF}}{\left(1 + K_{HMF} \cdot C_{HMF} + \sqrt{K_H \cdot C_{H2}} + K_{BHMF} \cdot C_{BHMF} + K_{DHMDHF} \cdot C_{DHMDHF} + K_{DHMTHF} \cdot C_{DHMTHF}\right)^3} \cdot \omega \quad (1)$$

$$R_2 = \frac{k_2 \cdot K_{BHMF} \cdot K_H \cdot C_{H2} \cdot C_{BHMF}}{\left(1 + K_{HMF} \cdot C_{HMF} + \sqrt{K_H \cdot C_{H2}} + K_{BHMF} \cdot C_{BHMF} + K_{DHMDHF} \cdot C_{DHMDHF} + K_{DHMTHF} \cdot C_{DHMTHF}\right)^3} \cdot \omega \quad (2)$$

$$R_3 = \frac{k_3 \cdot K_{DHMDHF} \cdot K_H \cdot C_{H2} \cdot C_{DHMDHF}}{\left(1 + K_{HMF} \cdot C_{HMF} + \sqrt{K_H \cdot C_{H2}} + K_{BHMF} \cdot C_{BHMF} + K_{DHMDHF} \cdot C_{DHMDHF} + K_{DHMTHF} \cdot C_{DHMTHF}\right)^3} \cdot \omega \quad (3)$$

where, k_i represents the rate constant for each reaction step i, K_j is the adsorption constant for each species j, C_j is the concentration of the species j, and ω is the catalyst loading in mass per reaction volume. Due to its properties, synthetic runs were performed using GVL as a solvent [38]. Table 1 displays the hypothetical true kinetic constants assigned and used in this study.

A modified Arrhenius equation was used as suggested by Buzzi-Ferraris [39].

$$\ln\left(k_i(T)\right) = \ln\left(k_i\left(T_{Ref}\right)\right) + \frac{E_{a,i}}{R \cdot T_{ref}} \cdot \left(1 - \frac{T_{Ref}}{T}\right) \quad (4)$$

where, $E_{a,i}$ is the activation of reaction i, R is the universal gas constant, T_{ref} is a reference temperature and T is the reaction temperature. Using Eq. (4) decreases the correlation between the rate constant and activation energy.

We also modified the adsorption constant as $\ln\left(K_j\right)$. In this way, we can linearize the numerator in Eqs (5) to (7).

Numerator parts were expressed as

$$k_1 \cdot K_{HMF} \cdot K_H = exp\left(\ln\left(k_1\left(T_{Ref}\right)\right) + \frac{E_{a,1}}{R \cdot T_{ref}} \cdot \left(1 - \frac{T_{Ref}}{T}\right) + \ln(K_{HMF}) + \ln(K_H)\right) \quad (5)$$

$$k_2 \cdot K_{BHMF} \cdot K_H = exp\left(\ln\left(k_2\left(T_{Ref}\right)\right) + \frac{E_{a,2}}{R \cdot T_{ref}} \cdot \left(1 - \frac{T_{Ref}}{T}\right) + \ln(K_{BHMF}) + \ln(K_H)\right) \quad (6)$$

$$k_3 \cdot K_{DHMDHF} \cdot K_H = exp\left(\ln\left(k_3\left(T_{Ref}\right)\right) + \frac{E_{a,3}}{R \cdot T_{ref}} \cdot \left(1 - \frac{T_{Ref}}{T}\right) + \ln(K_{DHMDHF}) + \ln(K_{DH})\right) \quad (7)$$

Table 1. Hypothetical true kinetic constants for the hydrogenation of 5-HMF over a virtual catalyst.

k_1(393.15K)	$4.00 \cdot 10^{-04}$	$\mathrm{mol} \cdot \mathrm{g}_{\mathrm{cat}}^{-1} \cdot \mathrm{s}^{-1}$
Ea_1	110	$\mathrm{kJ} \cdot \mathrm{mol}^{-1}$
k_2(393.15K)	$7.50 \cdot 10^{-05}$	$\mathrm{mol} \cdot \mathrm{g}_{\mathrm{cat}}^{-1} \cdot \mathrm{s}^{-1}$
Ea_2	130	$\mathrm{kJ} \cdot \mathrm{mol}^{-1}$
k_3(393.15K)	$4.80 \cdot 10^{-05}$	$\mathrm{mol} \cdot \mathrm{g}_{\mathrm{cat}}^{-1} \cdot \mathrm{s}^{-1}$
Ea_3	150	$\mathrm{kJ} \cdot \mathrm{mol}^{-1}$
K_{HMF}	0.8	$\mathrm{L} \cdot \mathrm{mol}^{-1}$
K_{BHMF}	0.4	$\mathrm{L} \cdot \mathrm{mol}^{-1}$
K_{DHMDHF}	0.3	$\mathrm{L} \cdot \mathrm{mol}^{-1}$
K_{DHMTHF}	0.1	$\mathrm{L} \cdot \mathrm{mol}^{-1}$
K_{H2}	10	$\mathrm{L} \cdot \mathrm{mol}^{-1}$

Table 2 displays the reaction enthalpies for each reaction step. These values were obtained from the study of Vasiliu et al. [40] at 298K. They calculated the hydrogenation enthalpy of BHMF to DHMTHF to be -155.64 $kJ \cdot mol^{-1}$, and we assumed that the enthalpy of each step was -77.82 $kJ \cdot mol^{-1}$. The choice of this reaction system was motivated by its multiphasic feature and the number of exothermic reaction steps.

Table 2. Reaction enthalpy values, calculated at 298K, at stake for the hydrogenation of 5-HMF to DHMTHF. [40]

Reaction steps	Reaction enthalpy $(\mathrm{kJ} \cdot \mathrm{mol}^{-1})$
R_1: HMF+H_2➔BHMF	-87.44
R_2: BHMF+H_2➔DHMDHF	-77.82
R_3: DHMDHF +H_2➔DHMTHF	-77.82

The kinetic model was developed in a batch reactor under isobaric mode. Synthetic runs were generated in isothermal or adiabatic conditions.

Material balances for the different species in the liquid phase are derived as

$$\frac{d[5-HMF]}{dt} = -R_1 \quad (8)$$

$$\frac{d[H_2]_{liq}}{dt} = k_L.a * \left([H_2]^*_{liq} - [H_2]_{liq}\right) - R_1 - R_2 - R_3 \quad (9)$$

$$\frac{d[BHMF]}{dt} = R_1 - R_2 \quad (10)$$

$$\frac{d[DHMDHF]}{dt} = R_2 - R_3 \quad (11)$$

$$\frac{d[DHMTHF]}{dt} = R_3 \quad (12)$$

where, $[H_2]^*_{liq}$ is the concentration of hydrogen at the gas-liquid interface. This concentration was determined using Henry's constant $He(T) = \frac{[H_2]^*_{liq}}{P_{H_2,Reactor}}$ (mol·L^{-1}·bar^{-1}).

The term $k_L.a$ is the volumetric gas-to-liquid mass transfer coefficient for hydrogen (s^{-1}), and was calculated as [41]

$$k_L.\mathrm{a} = (k_L.\mathrm{a})_{modified} * \left(\frac{T_{Liq}}{\mu_{Liq}}\right)^{0.5} * \left(\frac{\rho_{Liq}}{\mu_{Liq}}\right)^{0.25} \quad (13)$$

where, $(k_L.\mathrm{a})_{modified}$ was assumed constant for all the synthetic runs and fixed to $2.22 \cdot 10^{-6}\ \left(\frac{Pa \cdot s}{K}\right)^{0.5} \cdot \left(\frac{Pa \cdot s}{kg \cdot m^{-3}}\right)^{0.25} \cdot s^{-1}$. The temperature dependence of the density and kinematic viscosity of GVL, the solvent, was expressed via the data obtained from the work of Ariba et al. [42].

The equation of Van't Hoff was used to express Henry's temperature dependence:

$$He(T_R) = He\left(T_{Ref} = 373.15K\right) * exp\left(\frac{-\Delta H_{Sol.}}{R} * \left(\frac{1}{T_R} - \frac{1}{373.15}\right)\right) \quad (14)$$

From Wang et al. [41], it was found that $\Delta H_{Sol.H2} = 5936.8$ J·mol^{-1} and $He(T_{Ref} = 373.15K) =$ 1.86 mol·L^{-1}·bar^{-1}.

In the case of adiabatic synthetic runs, the thermal balance of the reaction system was included

$$\frac{\mathrm{d}T_R}{dt} = \frac{(-R_1 \cdot \Delta H_{R,1} - R_2 \cdot \Delta H_{R,2} - R_3 \cdot \Delta H_{R,3}) \cdot V}{m_R \cdot C_{PR} + m_{catalyst} \cdot Cp_{catalyst}} \quad (15)$$

where, T_R is the reaction temperature, R_i is the reaction rate of i, $\Delta H_{R,i}$ is the reaction enthalpy of i, m_R is the mass of the reaction mixture, C_{PR} is the heat capacity of the reaction mixture and was supposed to be one of the GVL solvent, $m_{catalyst}$ is the mass of catalyst, $Cp_{catalyst}$ is the heat capacity of the catalyst, and V is the reaction volume. The evolution of heat capacity and reaction volume with temperature was considered, and it was supposed to be one of the GVL solvents [42]. For the virtual catalyst, we used the heat capacity of activated carbon [43].

Synthetic data in isothermal and adiabatic conditions were generated from the resolution of ordinary differential equations (8) to (12) and (15) using kinetic and thermodynamic data from Tables 1 and 2. These ODEs were solved by DDAPLUS solver using a modified Newton algorithm [44], installed in the software Athena Visual Studio [45].

2.2 Generation of synthetic data with errors

This section describes the design of the experimental matrix created via the kinetic and thermodynamic constants (Tables 1 and 2). In the case of adiabatic runs, we added errors on concentration (initial and final) and reaction temperature.

Two types of synthetic data were generated: one with low error and the other with high error. One can find these data at Mendeley data presented in Excel files named: Synthetic_data_high_error_adiabatic; Synthetic_data_high_error_isothermal; Synthetic_data_low_error_adiabatic and Synthetic_data_low_error_isothermal (https://data.mendeley.com/datasets/v38n3wbsrt/1).

The level of errors was the ones typically found in the literature. We used the np.random.normal from Python.

2.2.1 Synthetic runs with low errors

Tables 3 and 4 display the experimental matrix for synthetic runs performed in isothermal and adiabatic conditions. These runs were generated using the initial conditions from Tables 3 and 4. An error with a standard deviation 5% was applied on concentration and 0.1 K for reaction temperatures (Excel files Synthetic_data_low_error_isothermal and Synthetic_data_low_error_adiabatic at https://data.mendeley.com/datasets/v38n3wbsrt/1). From laboratory experiments performed in adiabatic mode, it is not recommended to withdraw samples during the reaction to keep the reaction temperature signal stable. Therefore, there were no concentration values during the reaction for synthetic runs in adiabatic mode. Figures 2 and 3 show the true concentration of species and temperatures versus the noised-corrupted signals.

The design of the experimental matrix was done as the kinetic experimentalist model would have done. For instance, Runs 1 and 2; 3 and 4 were carried out to evaluate the effect of reaction temperature, Runs 3 and 5 to evaluate the effect of pressure; Runs 2 and 6 to evaluate the effect of catalyst loading; and Runs 1 and 7 to evaluate the effect of HMF loading.

Table 3. Experimental matrix for isothermal conditions with low error level.

Run	Temperature	m_{HMF0}	m_{GVL0}	m_{cat}	P_{H2}	$[GVL]_0$	$[H_2]_0$	$[DHMDHF]_0$	$[HMF]_0$	$[BHMF]_0$	$[DHMTHF]_0$
	°C	g			bar	$mol \cdot L^{-1}$					
1	100	4	30	0.08	50	8.62	0.00	0.00	0.91	0.00	0.00
2	110	4	30	0.08	50	8.54	0.00	0.00	0.90	0.00	0.00
3	130	4	30	0.02	50	8.37	0.00	0.00	0.89	0.00	0.00
4	160	4	30	0.02	50	8.12	0.00	0.00	0.86	0.00	0.00
5	130	4	30	0.02	20	8.37	0.00	0.00	0.89	0.00	0.00
6	110	4	30	1	50	8.54	0.00	0.00	0.90	0.00	0.00
7	100	1	30	0.08	50	9.46	0.00	0.00	0.25	0.00	0.00
8	110	3	30	0.06	30	8.80	0.00	0.00	0.70	0.00	0.00
9	160	10	30	0.005	100	6.91	0.00	0.00	1.83	0.00	0.00
10	140	10	30	0.004	80	7.05	0.00	0.00	1.86	0.00	0.00
11	140	6	30	0.3	70	7.83	0.00	0.00	1.24	0.00	0.00
12	150	8	30	0.15	90	7.34	0.00	0.00	1.55	0.00	0.00
13	120	10	30	0.25	100	7.19	0.00	0.00	1.90	0.00	0.00
14	150	8	30	0.35	90	7.34	0.00	0.00	1.55	0.00	0.00
15	150	10	30	0.25	100	6.98	0.00	0.00	1.85	0.00	0.00

Table 4. Experimental matrix for adiabatic conditions with low error level.

Run	Temperature	m_{HMF0}	m_{GVL0}	m_{cat}	P_{H2}	$[GVL]_0$	$[H_2]_0$	$[DHMDHF]_0$	$[HMF]_0$	$[BHMF]_0$	$[DHMTHF]_0$
	°C	g			bar	$mol \cdot L^{-1}$					
16	100	4	30	0.08	50	8.62	0.00	0.00	0.91	0.00	0.00
17	110	4	30	0.08	50	8.54	0.00	0.00	0.90	0.00	0.00
18	130	4	30	0.02	50	8.37	0.00	0.00	0.89	0.00	0.00
19	160	4	30	0.02	50	8.12	0.00	0.00	0.86	0.00	0.00
20	130	4	30	0.02	20	8.37	0.00	0.00	0.89	0.00	0.00
21	110	4	30	1	50	8.54	0.00	0.00	0.90	0.00	0.00
22	100	1	30	0.08	50	9.46	0.00	0.00	0.25	0.00	0.00
23	110	3	30	0.06	30	8.80	0.00	0.00	0.70	0.00	0.00
24	160	10	30	0.005	100	6.91	0.00	0.00	1.83	0.00	0.00
25	140	10	30	0.004	80	7.05	0.00	0.00	1.86	0.00	0.00

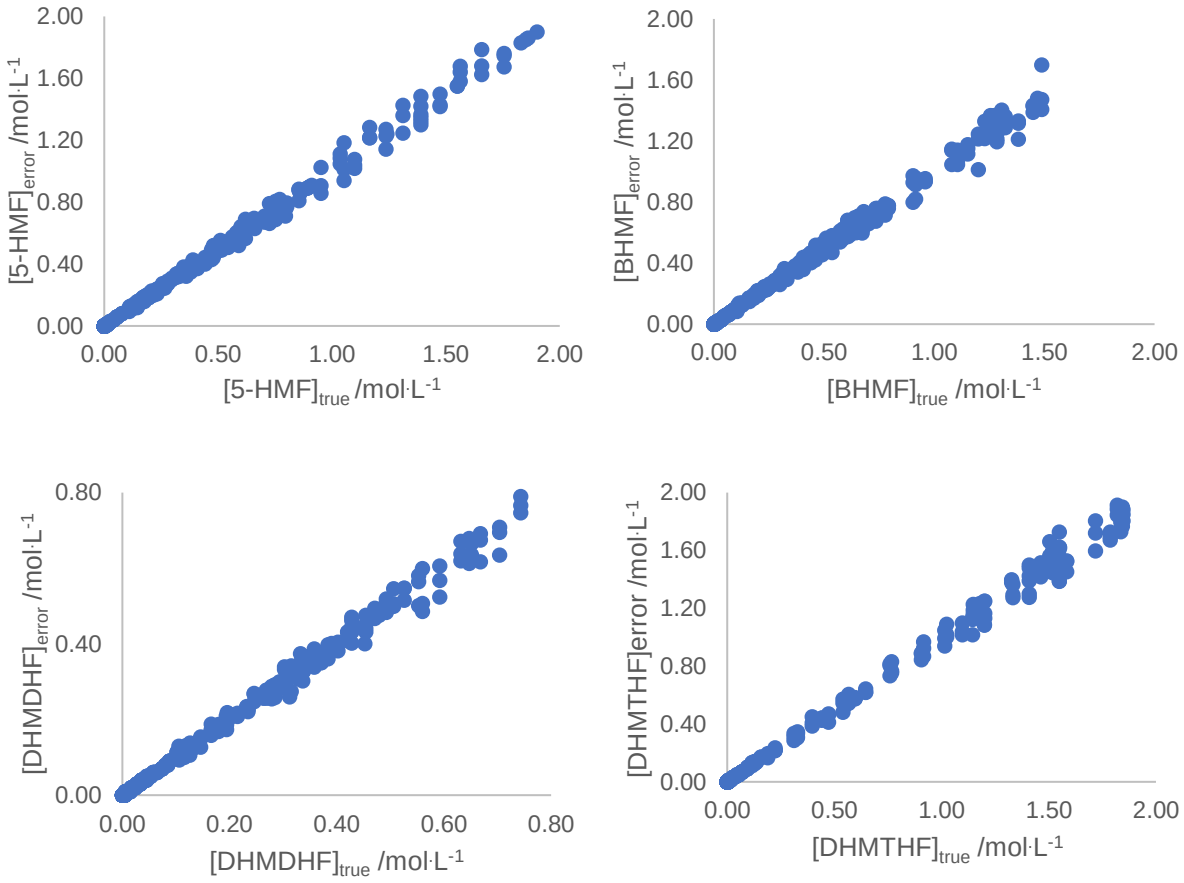

Figure 2. $[j]_{error}$ versus $[j]_{true}$ for runs carried out in isothermal mode (Runs 1 to 15).

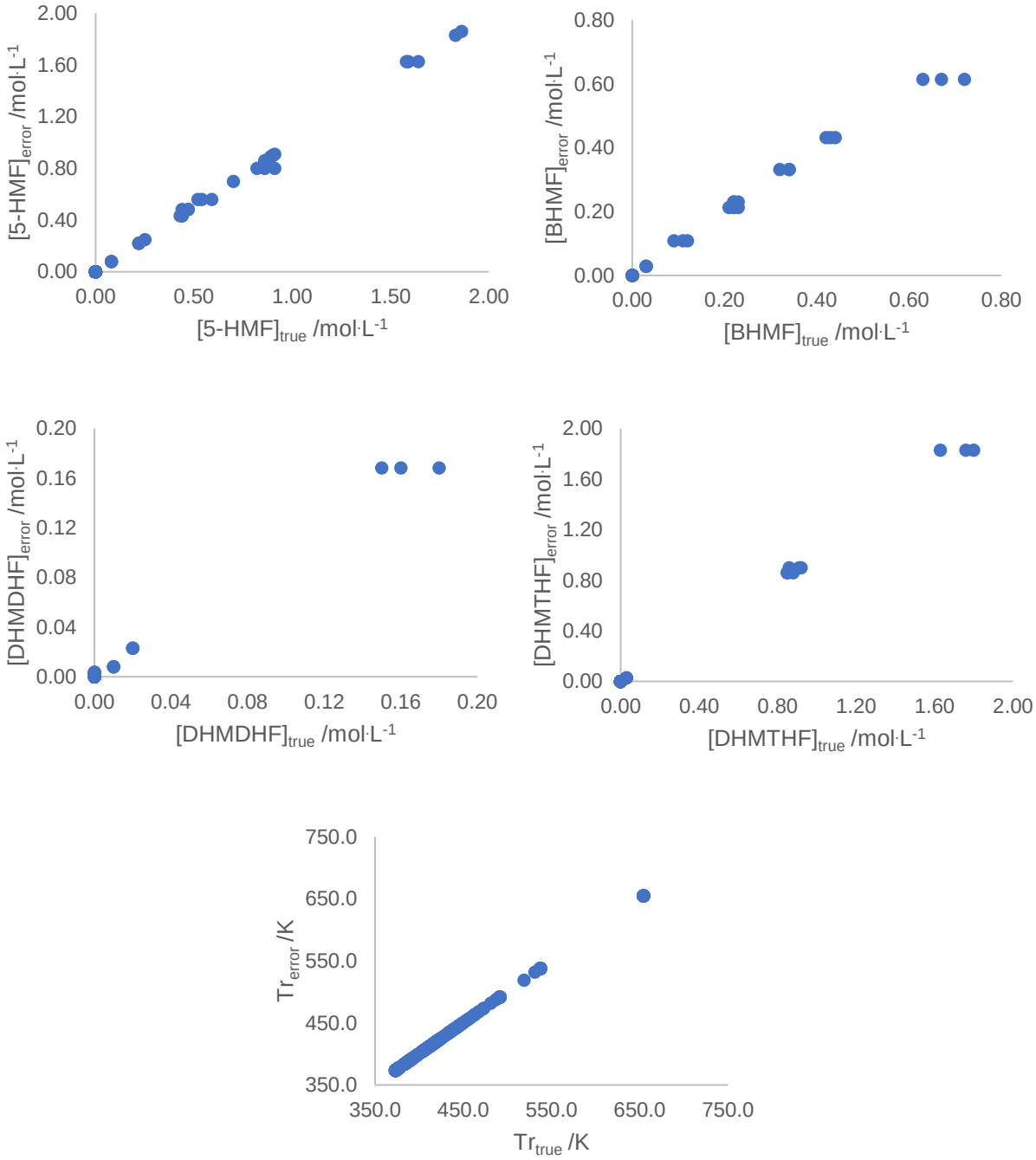

Figure 3. $[i]_{error}$ and $Tr,_{error}$ versus $[i]_{true}$ and $Tr,_{true}$ for runs carried out in adiabatic mode (Runs 16 to 25).

The impact of the number of adiabatic runs on kinetic model results was evaluated by using different synthetic runs:

-Approach1: all isothermal and adiabatic synthetic runs were used in the modeling stage, i.e., from Run 1 to Run 25;

-Approach2: all isothermal synthetic runs were used in the modeling stage, i.e., from Run 1 to Run 15;

-Approach3: all adiabatic synthetic runs were used in the modeling stage, i.e., from Runs 16 to 25;

-Approach4: 15 synthetic runs were used in the modeling stage, including 14 isothermal runs and 1 adiabatic run. We carried out modeling on 10 sets of runs (Supporting information, S1). The distribution between isothermal and adiabatic runs was done aleatory;

-Approach5: 15 synthetic runs were used in the modeling stage, including 13 isothermal runs and 2 adiabatic runs. We carried out modeling on 10 sets of runs (Supporting information, S1). The distribution between isothermal and adiabatic runs was done aleatory;

-Approach6: 15 synthetic runs were used in the modeling stage, including 10 isothermal runs and 5 adiabatic runs. We carried out modeling on 10 sets of runs (Supporting information, S1). The distribution between isothermal and adiabatic runs was done aleatory;

-Approach7: 15 synthetic runs were used in the modeling stage, including 9 isothermal runs and 6 adiabatic runs. We carried out modeling on 10 sets of runs (Supporting information, S1) to avoid false conclusions. The distribution between isothermal and adiabatic runs was done aleatory;

-Approach8: 15 synthetic runs were used in the modeling stage, including 7 isothermal runs and 8 adiabatic runs. We carried out modeling on 10 sets of runs (Supporting information, S1). The distribution between isothermal and adiabatic runs was done aleatory.

For Approaches 4 to 8, different sets of runs were evaluated to avoid drawing hasty conclusions. All modeling results are Mendeley data (https://data.mendeley.com/datasets/v38n3wbsrt/1 and Excel files : Kinetic_modeling_Approach1_All_isothermal_adiabatic_experiments_LHD1_low_errors; Kinetic_modeling_Approach2_All_isothermal_experiments_LHD1_low_errors; Kinetic_modeling_Approach3_All_adiabatic_experiments_LHD1_low_errors; Kinetic_modeling_Approach4_14_isothermal_1_adiabatic_runs_LHD1_low_errors; Kinetic_modeling_Approach5_13_isothermal_2_adiabatic_runs_LHD1_low_errors; Kinetic_modeling_Approach6_10_isothermal_5_adiabatic_runs_LHD1_low_errors; Kinetic_modeling_Approach7_9_isothermal_6_adiabatic_runs_LHD1_low_errors and Kinetic_modeling_Approach8_9_isothermal_8_adiabatic_runs_LHD1_low_errors.

2.2.2 Synthetic runs with high errors

Tables 5 and 6 display the experimental matrix for synthetic runs performed in isothermal and adiabatic conditions. Initial conditions were used to create synthetic data at high errors. An error with a standard deviation 13% was applied on concentration and 1K for reaction temperatures (Excel files Synthetic_data_high_error_isothermal and Synthetic_data_high_error_adiabatic at https://data.mendeley.com/datasets/v38n3wbsrt/1). No samples were withdrawn during the synthetic adiabatic runs. Figures 4 and 5 show the true concentration of species and temperatures versus the noised-corrupted signals.

Table 5. Experimental matrix for high error in isothermal conditions.

Run	Temperature	m_{HMF0}	m_{GVL0}	m_{cat}	P_{H2}	$[GVL]_0$	$[H_2]_0$	$[DHMDHF]_0$	$[HMF]_0$	$[BHMF]_0$	$[DHMTHF]_0$
	°C	g			bar	$mol \cdot L^{-1}$					
1 H	100	4	30	0.08	50	8.62	0	0	0.91	0	0
2 H	110	4	30	0.08	50	8.54	0	0	0.90	0	0
3 H	130	4	30	0.02	50	8.37	0	0	0.89	0	0
4 H	160	4	30	0.02	50	8.12	0	0	0.86	0	0
5 H	130	4	30	0.02	20	8.37	0	0	0.89	0	0
6 H	110	4	30	1	50	8.54	0	0	0.90	0	0
7 H	100	1	30	0.08	50	9.46	0	0	0.25	0	0
8 H	110	3	30	0.06	30	8.80	0	0	0.70	0	0
9 H	160	10	30	0.005	100	6.91	0	0	1.83	0	0
10 H	140	10	30	0.004	80	7.05	0	0	1.86	0	0
11 H	140	6	30	0.3	70	7.83	0	0	1.24	0	0
12 H	150	8	30	0.15	90	7.34	0	0	1.55	0	0
13 H	120	10	30	0.25	100	7.19	0	0	1.90	0	0
14 H	150	8	30	0.35	90	7.34	0	0	1.55	0	0
15 H	150	10	30	0.25	100	6.98	0	0	1.85	0	0
16 H	100	9	30	1.00	100	7.52	0	0	1.79	0	0
17 H	110	9	30	1.00	100	7.45	0	0	1.77	0	0
18 H	90	9	30	1.00	100	7.59	0	0	1.81	0	0
19 H	95	1	30	0.10	100	9.50	0	0	0.25	0	0
20 H	125	1	30	0.10	100	9.23	0	0	0.24	0	0

Table 6. Experimental matrix for high error in adiabatic conditions.

Run	Temperature	m_{HMF0}	m_{GVL0}	m_{cat}	P_{H2}	$[GVL]_0$	$[H_2]_0$	$[DHMDHF]_0$	$[HMF]_0$	$[BHMF]_0$	$[DHMTHF]_0$
	°C	g			bar	$mol \cdot L^{-1}$					
21H	100	4	30	0.08	50	8.62	0.00	0.00	0.91	0.00	0.00
22H	110	4	30	0.08	50	8.54	0.00	0.00	0.90	0.00	0.00
23H	130	4	30	0.02	50	8.37	0.00	0.00	0.89	0.00	0.00
24H	160	4	30	0.02	50	8.12	0.00	0.00	0.86	0.00	0.00
25H	130	4	30	0.02	20	8.37	0.00	0.00	0.89	0.00	0.00
26H	110	4	30	1.00	50	8.54	0.00	0.00	0.90	0.00	0.00
27H	100	1	30	0.08	50	9.46	0.00	0.00	0.25	0.00	0.00
28H	110	3	30	0.06	30	8.80	0.00	0.00	0.70	0.00	0.00
29H	160	10	30	0.01	100	6.91	0.00	0.00	1.83	0.00	0.00
30H	140	10	30	0.00	80	7.05	0.00	0.00	1.86	0.00	0.00
31H	90	7	30	1.20	30	8.00	0.00	0.00	1.48	0.00	0.00
32H	90	7	30	1.20	50	8.00	0.00	0.00	1.48	0.00	0.00
33H	90	7	30	1.20	70	8.00	0.00	0.00	1.48	0.00	0.00
34H	90	7	30	1.20	90	8.00	0.00	0.00	1.48	0.00	0.00
35H	95	7	30	0.50	90	7.96	0.00	0.00	1.48	0.00	0.00
36H	95	7	30	1.20	90	7.96	0.00	0.00	1.48	0.00	0.00
37H	127	8	30	0.05	95	7.52	0.00	0.00	1.59	0.00	0.00
38H	127	8	30	0.07	95	7.52	0.00	0.00	1.59	0.00	0.00
39H	127	8	30	0.14	95	7.52	0.00	0.00	1.59	0.00	0.00
40H	127	8	30	0.30	95	7.52	0.00	0.00	1.59	0.00	0.00

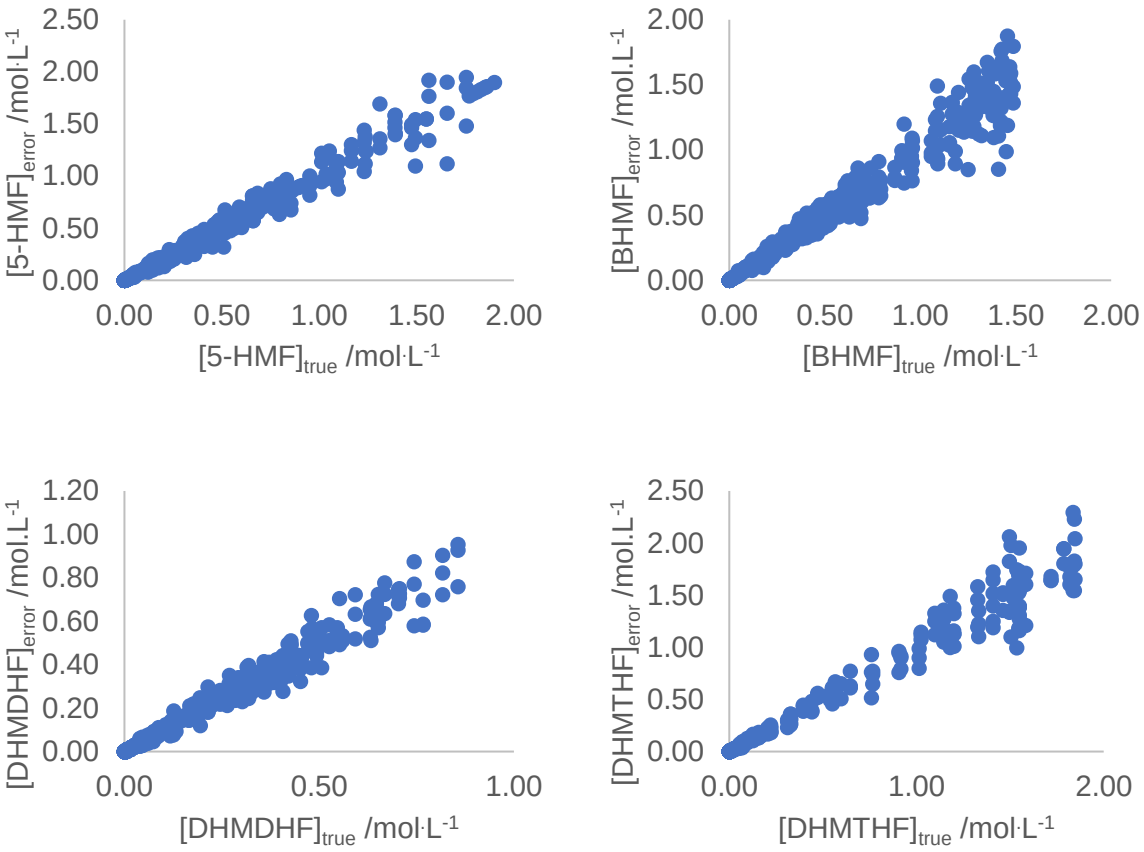

Figure 4. $[j]_{error}$ versus $[j]_{true}$ for runs carried out in isothermal mode (Runs 1H to 20H).

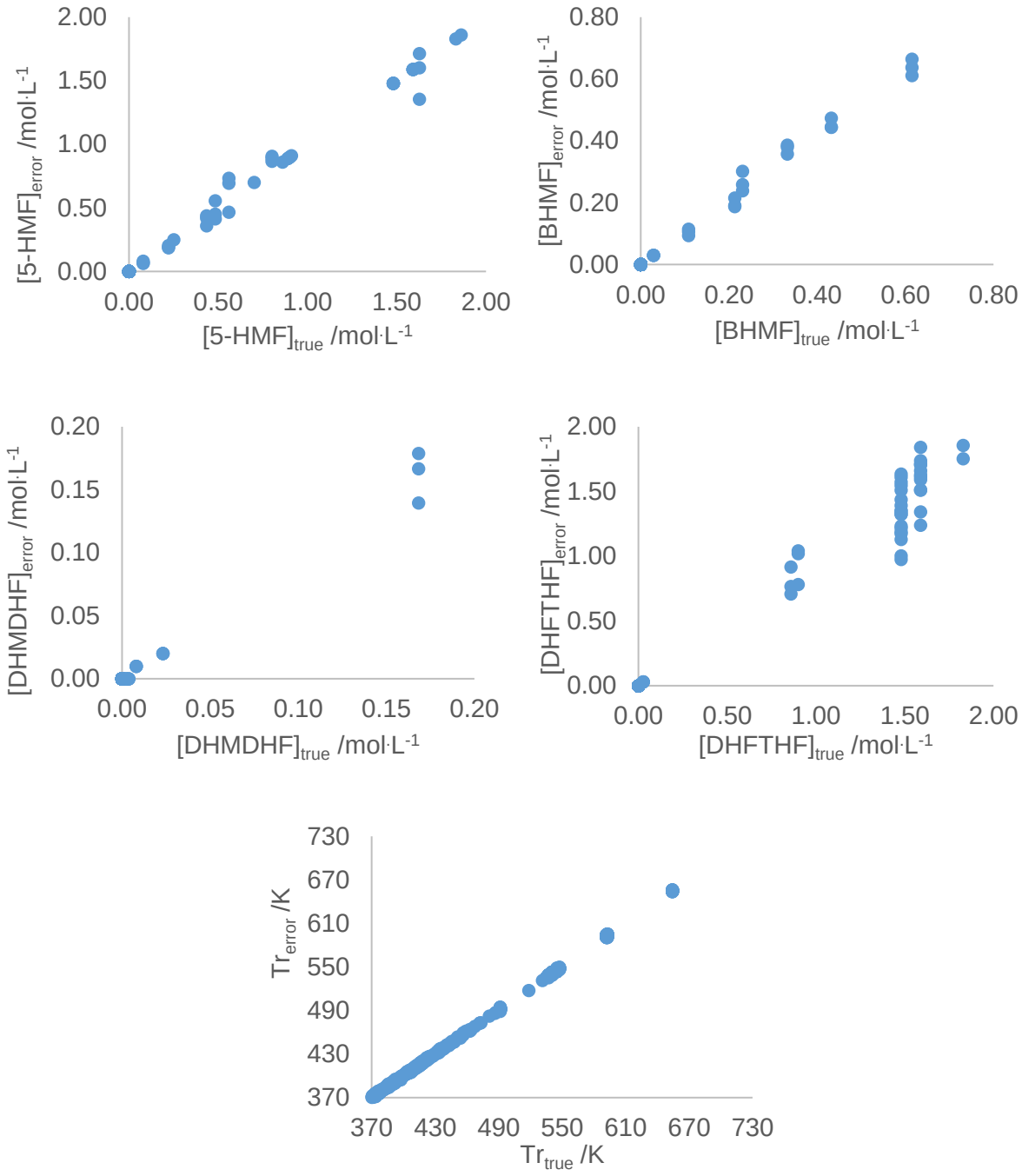

Figure 5. $[i]_{error}$ and $Tr_{,error}$ versus $[i]_{true}$ and $Tr_{,true}$ for runs carried out in adiabatic mode (Runs 21H to 40H).

As for synthetic runs with low errors, we make the kinetic modeling by using several approaches for synthetic runs with high errors (S3).

3 Sensitivity analysis using hypothetical true kinetic constants

A global sensitivity analysis was performed via Sobol's method based on the variance decomposition technique [46,47]. The SALib Python library was used [48].

The purpose of this analysis is to evaluate the impact of true kinetic constants (Table 1) and initial operating conditions on the ordinary differential equations (8)-(12) and (15). Such analysis is vital to know the difficulty of estimating some kinetic constants. In adiabatic conditions (Figure 6), one can notice that the natural logarithm of the first reaction step, mass catalyst and initial temperature has a significant influence on the concentration of HMF, BHMF, DHMTHF, DHMDHF, H_2 and reaction temperature. The other kinetic constants have a lower effect, which could make their estimation very challenging. One should remember that for adiabatic conditions, we track the concentrations at the beginning and end, and the reaction temperature during the reaction time.

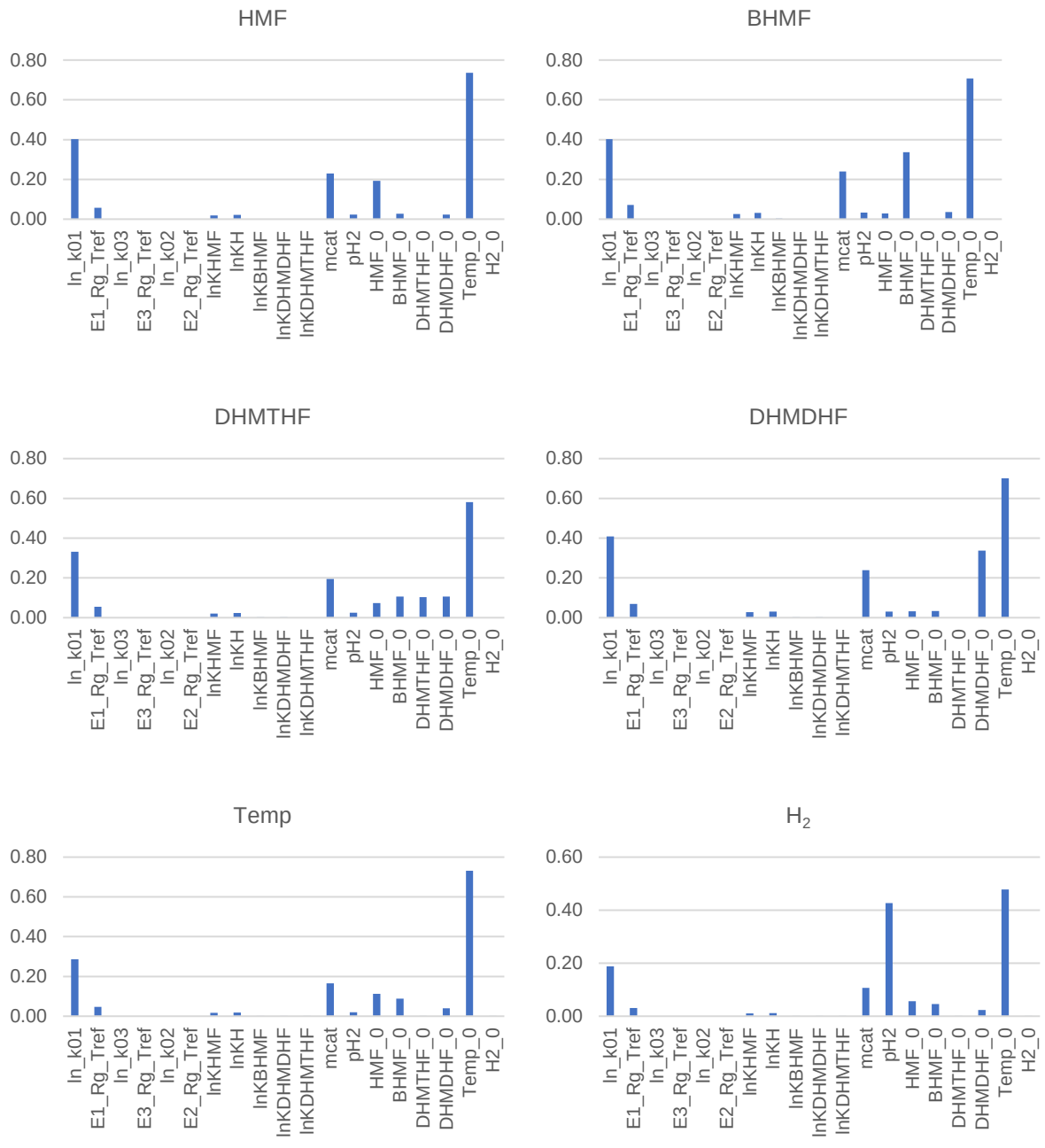

Figure 6. Sobol total-order sensitivity indices for adiabatic synthetic runs.

Figure 7 shows the Sobol total-order sensitivity indices for species concentration in isothermal conditions. The natural logarithm of the rate constant of the first reaction step significantly impacts the concentrations, except for the concentration of hydrogen. This observation is because we worked in isobaric and isothermal conditions; thus, the concentration of hydrogen stays constant with reaction time. The temperature and mass of the catalyst significantly impact

the different concentrations, except for hydrogen. One can also notice that the other kinetic constants do not significantly affect the concentration effect.

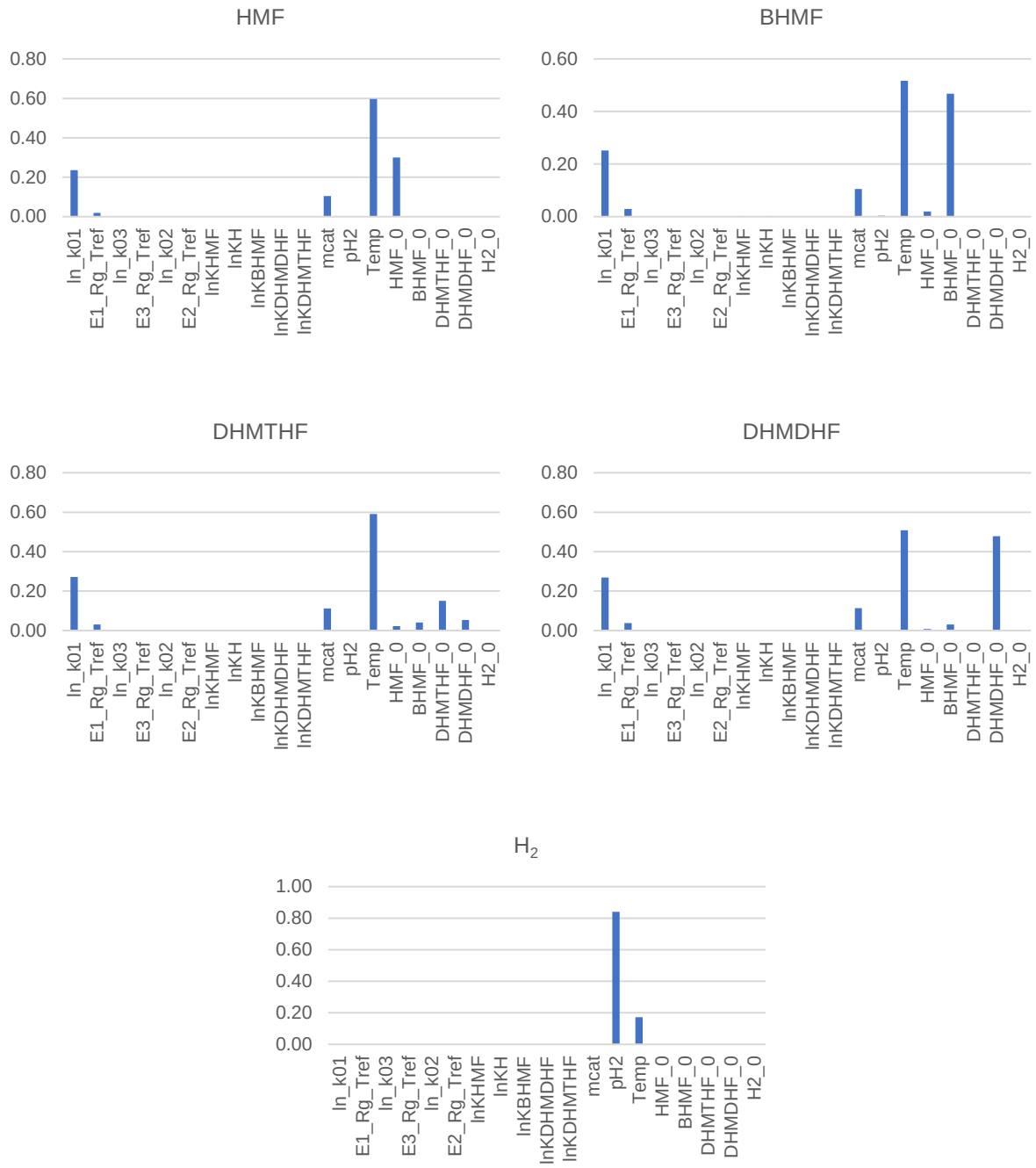

Figure 7. Sobol total-order sensitivity indices for isothermal synthetic runs.

4 Kinetic modeling using synthetic runs with errors

Non-linear regression was done via Athena Visual Studio software [45].

In isothermal conditions, the following observables were used as observables: 5-HMF, BHMF, DHMDHF, and DHMTHF concentrations. In adiabatic conditions, the initial and final concentrations were used as observables, and the reaction temperature was recorded at regular time intervals. Bayesian framework is more suitable for a multiresponse system than the non-linear least squares approach [49,50]. Indeed, Box and Draper developed a methodology to minimize the determinant criterion used as an objective function (OF) in the Bayesian framework in a multiresponse system [51,52].

The GREGPLUS subroutine, implemented in Athena Visual Studio, minimizes the OF [45,49]. This subroutine also determines the credible intervals for each estimated parameter and calculates the normalized parameter covariance. The OF is expressed by

$$OF = (\alpha + \beta + 1) \cdot \ln(|v|) \quad (16)$$

where $|v|$ is the determinant of the covariance matrix of the responses, β is the number of responses, and α is the number of events in response.

Each element of this matrix is as follows:

$$v_{ij} = \sum WF.(y_{iu} - \widehat{y_{iu}}) \cdot \left(y_{ju} - \widehat{y_{ju}}\right) \quad (17)$$

where y_{iu} is the synthetic concentration or temperature and $\widehat{y_{iu}}$ is the estimated value for response i and event u; and y_{ju} the synthetic data and $\widehat{y_{ju}}$ the estimated value for response j and event u. The term WF is the weight factor value.

The minimization of the OF is done via successive quadratic programming.

The credible intervals of the estimated parameters were evaluated by the marginal highest posterior density (HPD).

4.1 Kinetic modeling with synthetic runs with low errors

Figures 8 and 9 show examples of the fit of the model to the synthetic data. Approach 1 was used for these figures, i.e., all isothermal and adiabatic synthetic runs were used. The error bars represent the 95% confidence interval value and Student's t distribution. The variance σ^2 was calculated as

$$\sigma^2 = \frac{1}{n-1}\sum_{p=1}^{n}\left(x_p - \bar{x}\right)^2 \quad (18)$$

where, n is the number of replicates, x_p the concentration or temperature values of sample p and $\bar{x}$ is the mean value of the replicate. It was assumed that each sample was analyzed three times, for that reason there is three replicate values for the concentration.

The error bars were calculated as

$$\bar{x} - t_{\frac{\alpha}{2}}^{n-1} \cdot \frac{\sigma}{\sqrt{n}}, \bar{x} + t_{\frac{\alpha}{2}}^{n-1} \cdot \frac{\sigma}{\sqrt{n}} \quad (19)$$

$t_{\frac{\alpha}{2}}^{n-1}$ is the student t-value for n-1 samples.

Figure 8 shows that the fit of the model to synthetic data (mean value) is good; there was no temperature because it was done in isothermal conditions. Figure 9 shows that the fit of the model to synthetic concentration and temperature in adiabatic mode is good. Run 19 is an adiabatic synthetic run, so no samples were withdrawn during the reaction progress.

The results of kinetic modeling for Approach 1, including the correlation matrix and HPD intervals, could be found in the repository (Excel file Kinetic_modeling_Approach1_All_isothermal_adiabatic_experiments_LHD1_low_errors at https://data.mendeley.com/datasets/v38n3wbsrt/1).

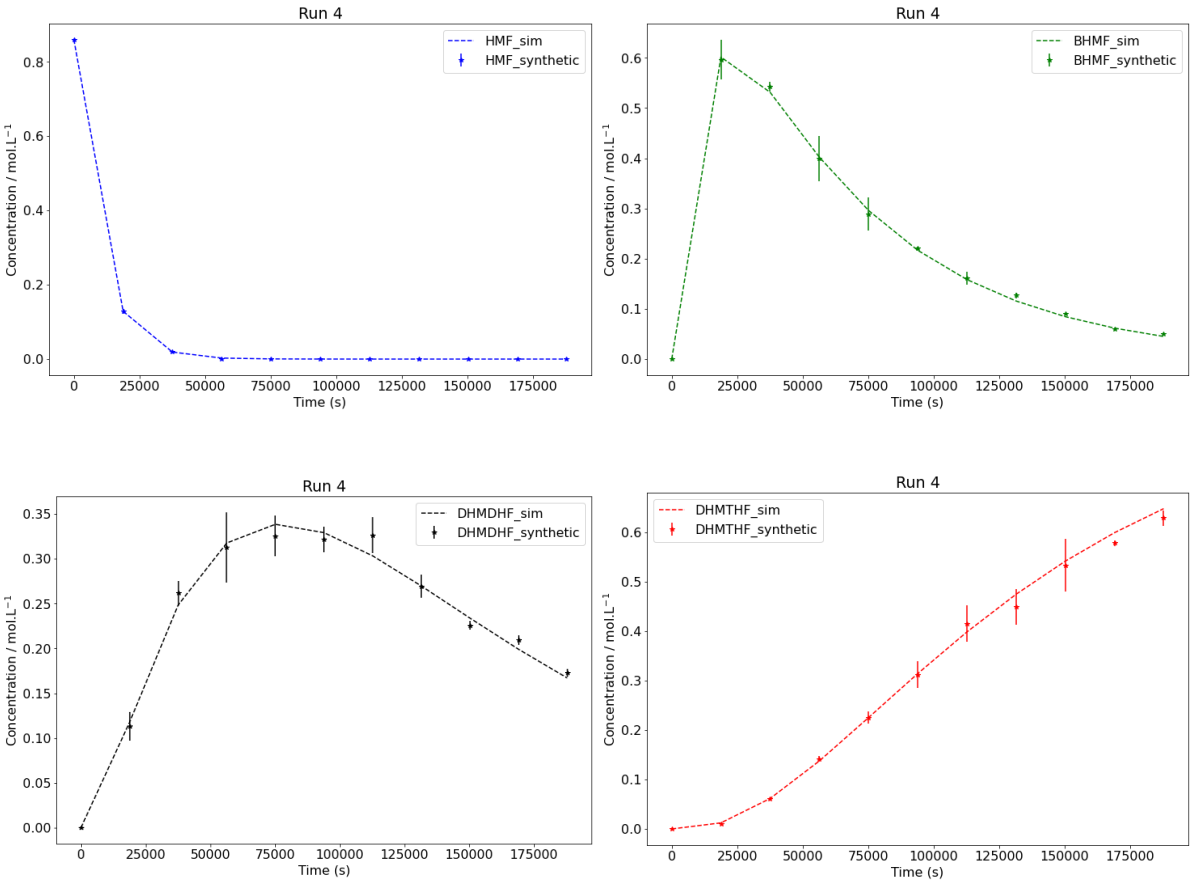

Figure 8. Fit of the model LHD1 to synthetic concentration with low error for synthetic Run 4 for Approach1 (error bars are 95% confidence interval).

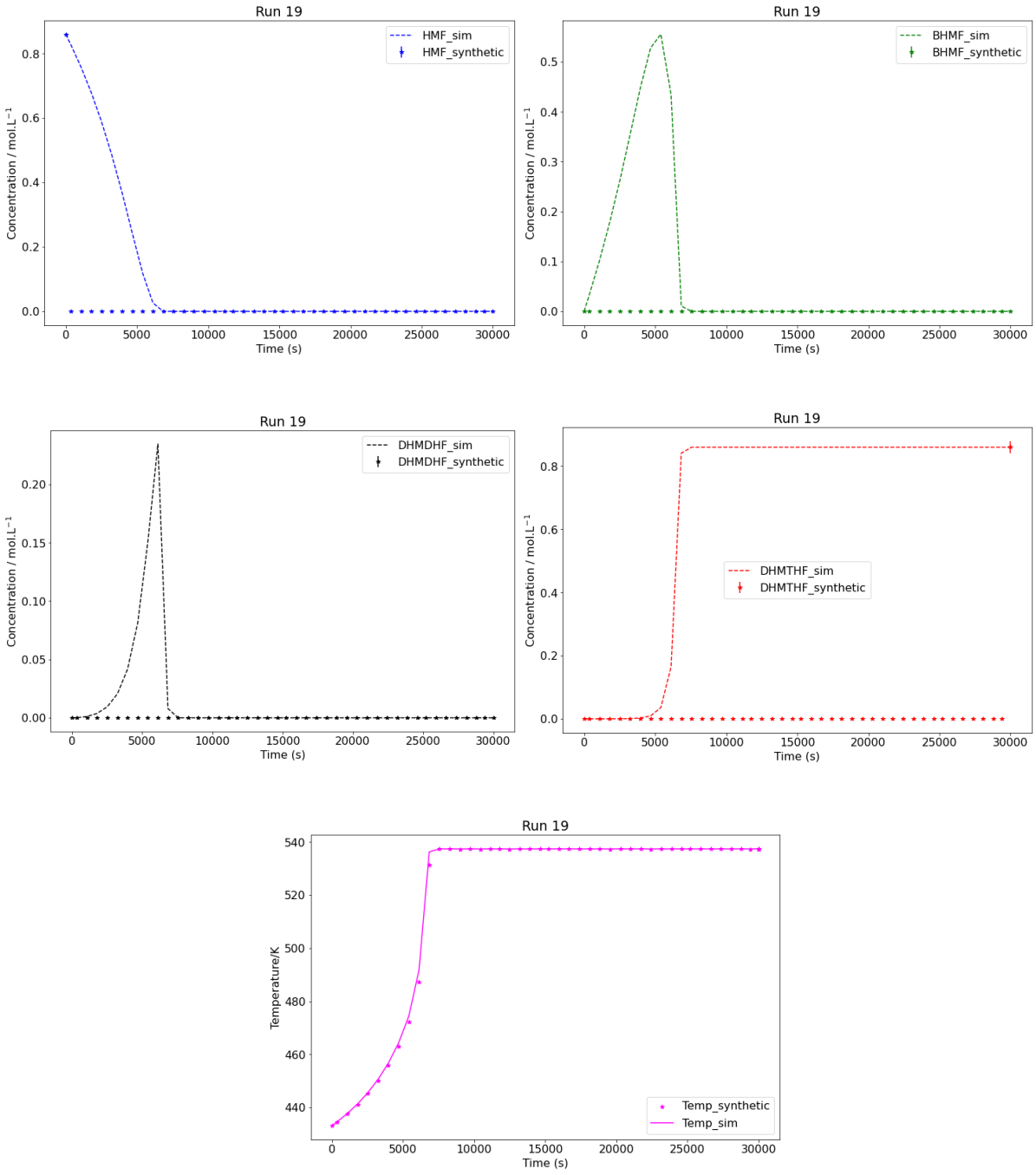

Figure 9. Fit of the model LHD1 to synthetic concentration with low error for synthetic Run 19 for Approach 1(error bars are 95% confidence interval)

Figure 10 shows the ratio SSR/n, where n represents the total synthetic point number. Approaches 1 to 3 were done with all Runs, all isothermal and all adiabatic runs, respectively. Therefore, no error bars were associated to their SSR/n values. Approaches 4 to 8 were performed using different sets of runs (Supporting information S1), thus, it was possible to calculate the error bars, based on the standard deviation. Figure 10 shows that all approaches give similar SSR/n values concentrations, except for Approach 3. Approach 3, only adiabatic synthetic runs, gives a high ratio for concentration and temperatures. It is interesting to observe that Approach 8, constituting 8 adiabatic and 7 isothermal runs, gave similar SSR/n values to Approach 1. Such an approach could be beneficial to decrease the number of isothermal runs, which are time-consuming for the analytical part.

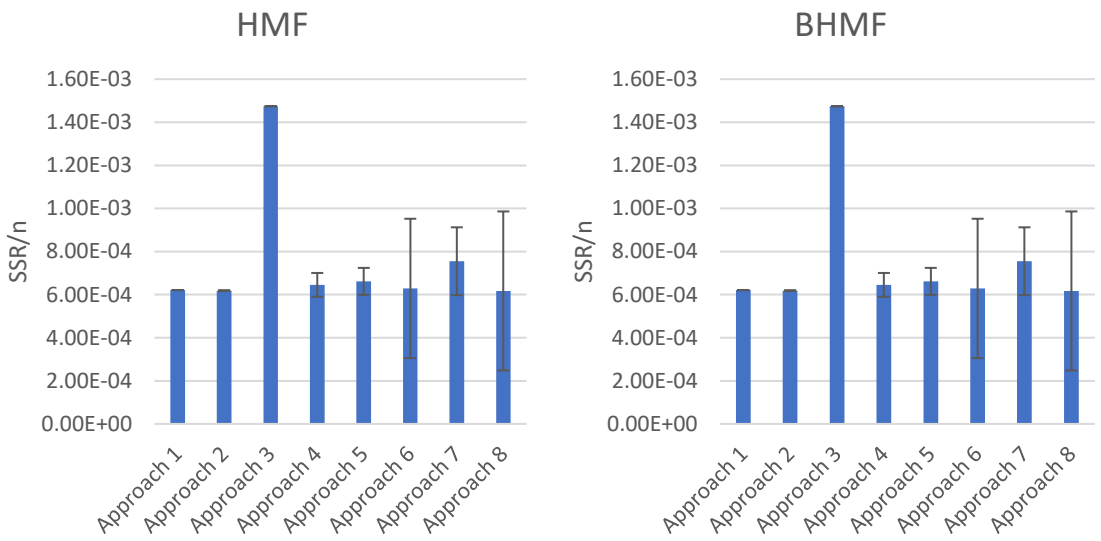

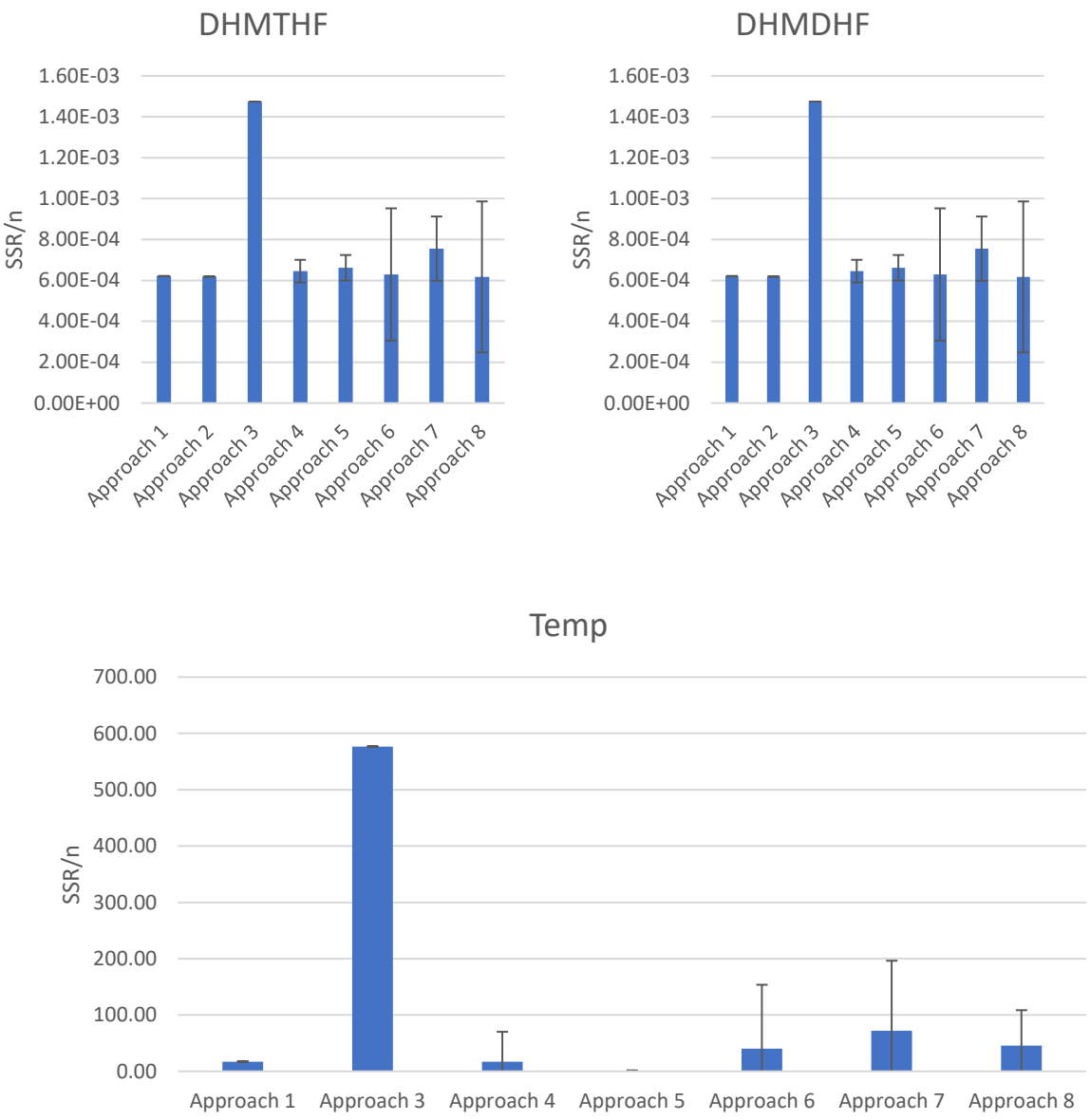

Figure 10. SSR/n with different approaches.

Figure 11 shows the estimated results for Approaches 1 to 3, i.e., using all synthetic runs, all isothermal synthetic runs and all adiabatic synthetic runs. The error bars represent the HPD values (Excel files Kinetic_modeling_Approach2_All_isothermal_experiments_LHD1_low_errors; Kinetic_modeling_Approach3_All_adiabatic_experiments_LHD1_low_errors; Summary_LHD1_low_errors at https://data.mendeley.com/datasets/v38n3wbsrt/1). The estimated parameters are generally similar to the hypothetical true ones for modeling using all numerical and isothermal synthetic runs. This observation is more nuanced for modeling using only all adiabatic synthetic runs (Approach 3). The regression time is longer using all adiabatic synthetic runs because they are more synthetic data, giving less accurate results for the logarithm of rate and adsorption constants.

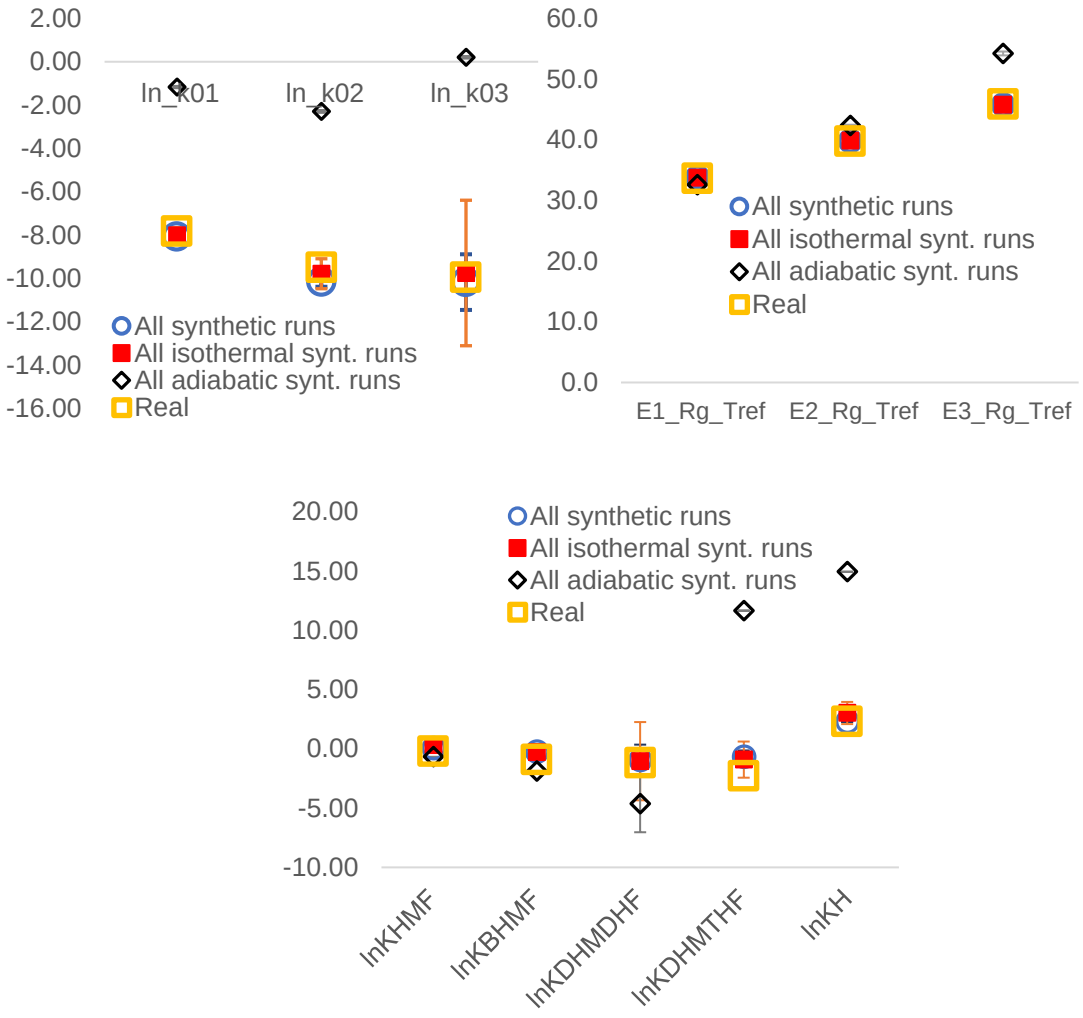

Figure 11. Comparison of the estimated kinetic constants obtained from Approach 1 to 3 (i.e., all synthetic runs, all isothermal synthetic runs and all adiabatic synthetic runs) and the hypothetical true ones (Real), where the error bars are the HPD intervals.

Table 7 recaps the different approaches with low errors.

Table 7. Number of adiabatic and isothermal synthetic runs in the approach.

Approach	Number of isothermal runs	Number of adiabatic runs
1	15	10
2	15	0
3	0	10
4	14	1
5	13	2
6	10	5
7	9	6
8	7	8

Figure 12 shows the effect of the number of adiabatic runs on the estimation of different kinetic constants. The total number of synthetic runs used in the modeling is 15. The orange line represents the true hypothetical values. The error bars do not represent the HPD but the standard deviation between each modeling (Supporting information S2 and Excel files Kinetic_modeling_ApproachX_All_isothermal_adiabatic_experiments_LHD1_low_errors and Summary_LHD1_low_errors at https://data.mendeley.com/datasets/v38n3wbsrt/1). For instance, for Approach 4, we performed the kinetic modeling for each Mix (Supporting information S1) thus, we got 10 values for each estimated kinetic constants.

In general, one can observe that modeling the different set of synthetic runs in the Approach (Supporting information S1-Approaches 4 to 8) can provide estimated kinetic constants close to the true hypothetical values. Nevertheless, one must conclude that parameter estimation using 15 isothermal synthetic runs with low errors gives estimated constants closer to the true hypothetical values.

From Figure 12, one cannot include that there is a clear effect of the number of adiabatic synthetic runs on the results of kinetic modeling. The error bars in Figure 12 are the standard deviation between each mix set of runs.

One should remember that the benefit of adiabatic synthetic runs compared to isothermal synthetic runs is that there are fewer samples to analyze.

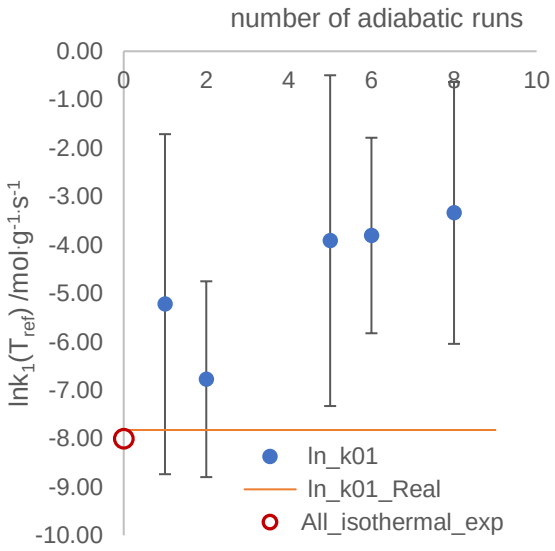

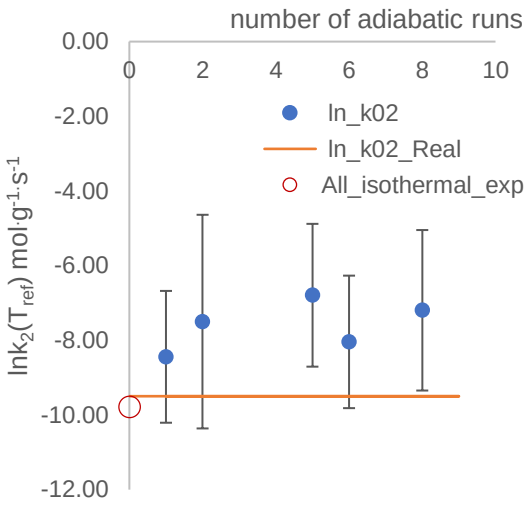

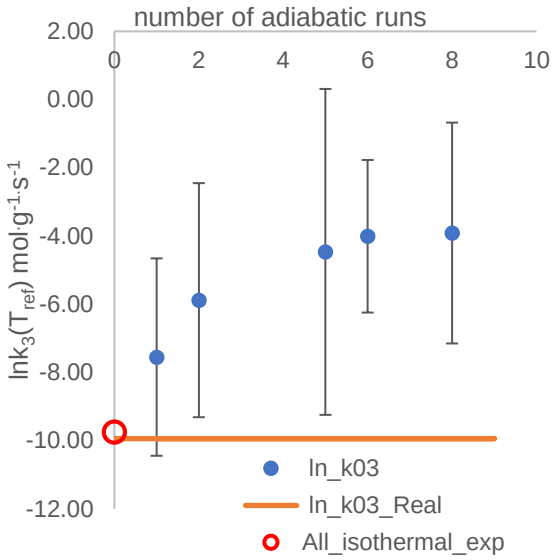
number of adiabatic runs
2.00
0.00
-2.00
-4.00
-6.00
-8.00
-10.00
-12.00
0
2
4
6
8
10
lnk3(Tref) mol·g-1·s-1
ln_k03
ln_k03_Real
All_isothermal_exp

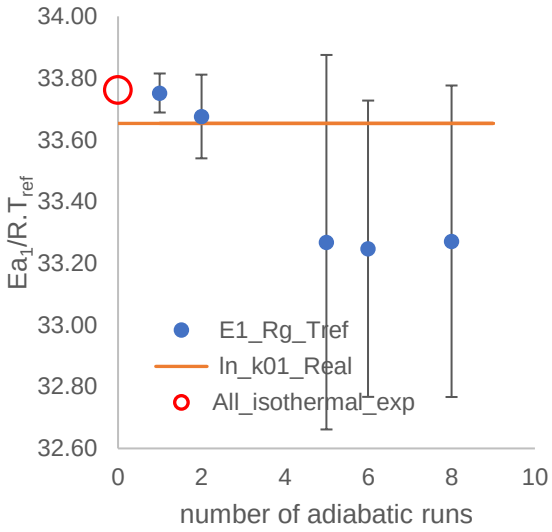
34.00
33.80
33.60
33.40
33.20
33.00
32.80
32.60
0
2
4
6
8
10
Ea1/R.Tref
E1_Rg_Tref
ln_k01_Real
All_isothermal_exp
number of adiabatic runs

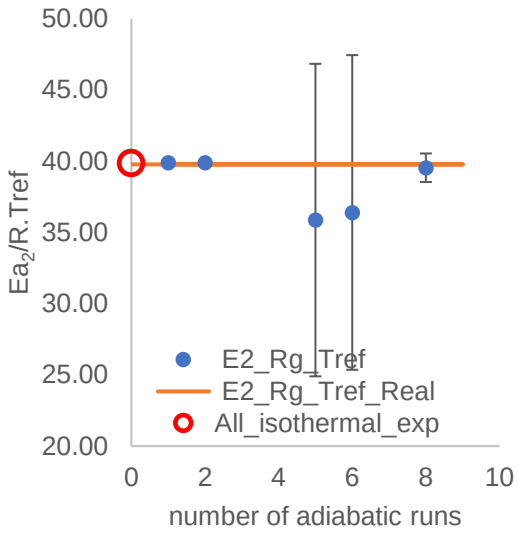
50.00
45.00
40.00
35.00
30.00
25.00
20.00
0
2
4
6
8
10
Ea2/R.Tref
E2_Rg_Tref
E2_Rg_Tref_Real
All_isothermal_exp
number of adiabatic runs

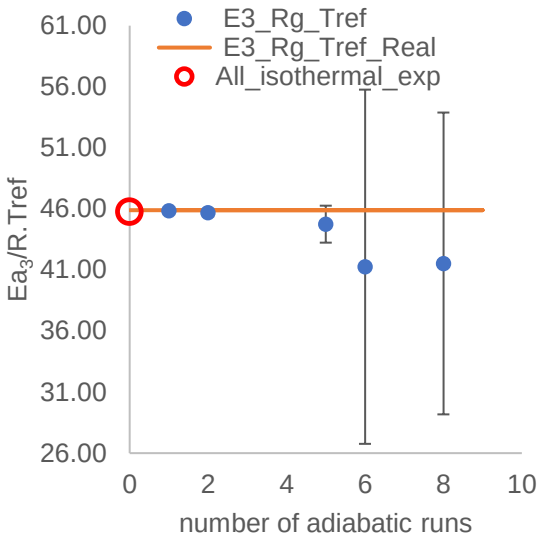
61.00
56.00
51.00
46.00
41.00
36.00
31.00
26.00
0
2
4
6
8
10
Ea3/R.Tref
E3_Rg_Tref
E3_Rg_Tref_Real
All_isothermal_exp
number of adiabatic runs

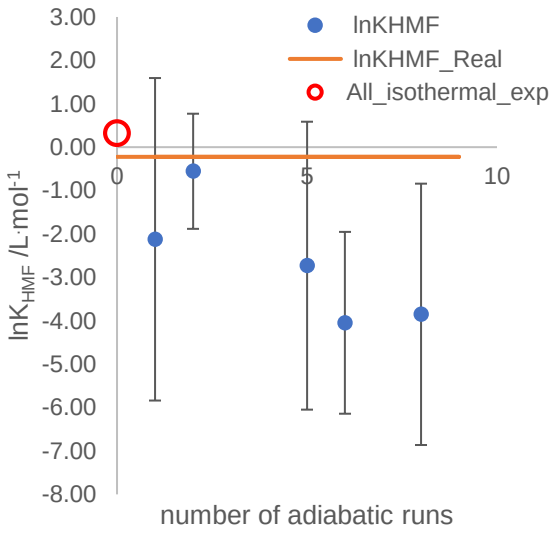
3.00
2.00
1.00
0.00
-1.00
-2.00
-3.00
-4.00
-5.00
-6.00
-7.00
-8.00
0
5
10
lnKHMF /L·mol-1
lnKHMF
lnKHMF_Real
All_isothermal_exp
number of adiabatic runs

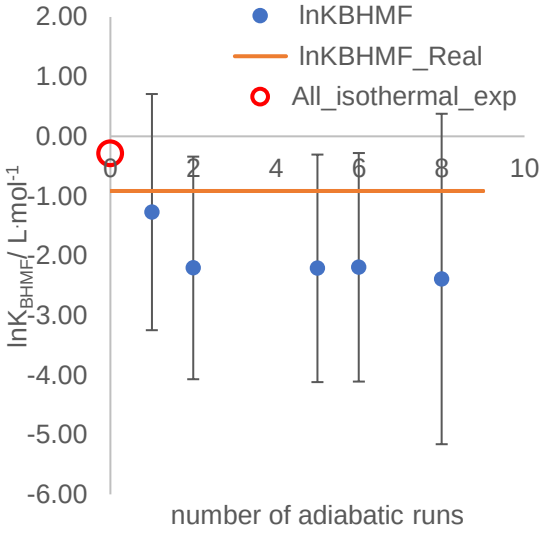
2.00
1.00
0.00
-1.00
-2.00
-3.00
-4.00
-5.00
-6.00
0
2
4
6
8
10
lnKBHMF/ L·mol-1
lnKBHMF
lnKBHMF_Real
All_isothermal_exp
number of adiabatic runs

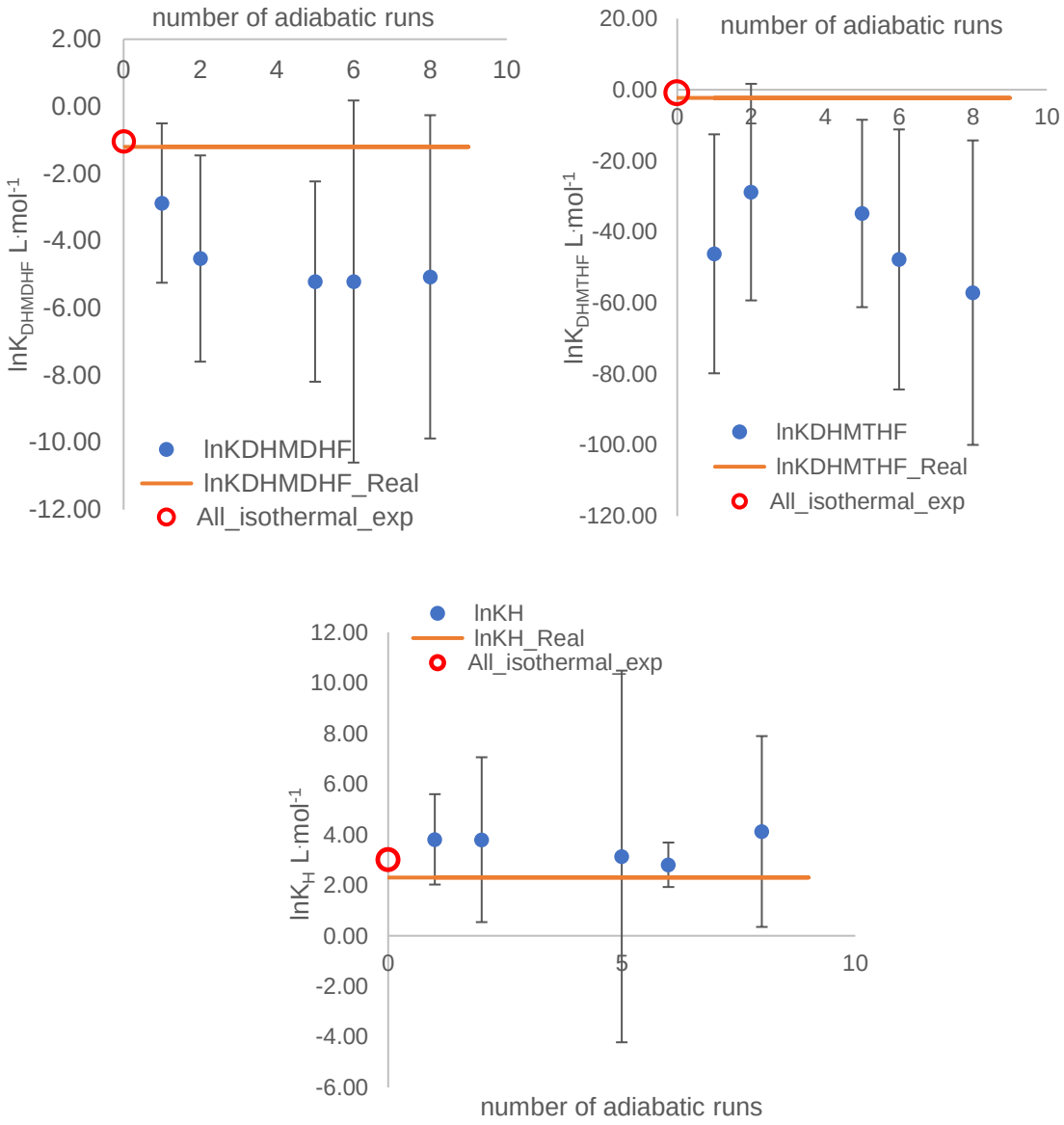

Figure 12. Effect of adiabatic synthetic runs with low errors for Approaches 2 (all isothermal runs) and 4 to 8 (error bars are the standard deviation) towards hypothetical true kinetic constants (Real).

We did not observe strong correlations between estimated parameters in kinetic models developed using low error. The analysis of the normalized covariance matrices did not show high values, i.e., higher than the absolute value of 0.95 [53]. The same observation was done by analyzing the parity plots for each observable, and it was found that the model can correctly

predict the synthetic data. The kinetic models are available in the repertory Mendeley Data (https://data.mendeley.com/datasets/v38n3wbsrt/1).

4.2 Kinetic modeling with synthetic runs with high errors.

We studied the effect of high error on the modeling. From the 20 synthetic runs generated in isothermal conditions (Table 5) and from the 20 synthetic runs generated in adiabatic conditions (Table 6), we evaluated 6 approaches summarized in Table 8. In Supporting information, S3 shows the aleatory distribution of the different runs for the different approaches.

Table 8. Number of adiabatic and isothermal synthetic runs in the Approach using synthetic runs with high errors.

Approach	Number of isothermal synthetic runs	Number of adiabatic synthetic runs
1H	20	0
2H	0	20
3H	17	3
4H	14	6
5H	10	10
6H	6	14

Figure 13 shows the fit of the model to synthetic concentrations (exp_mean) from Run17H in isothermal conditions via Approach 1H, where the error bars represent the confidence interval of 95%. One can notice that the model can fit the synthetic concentration in an excellent way. Figure 14 shows the fit of the model to synthetic concentrations (_exp) and reaction temperature (Temp_exp) for Run 40H via Approach 6H.

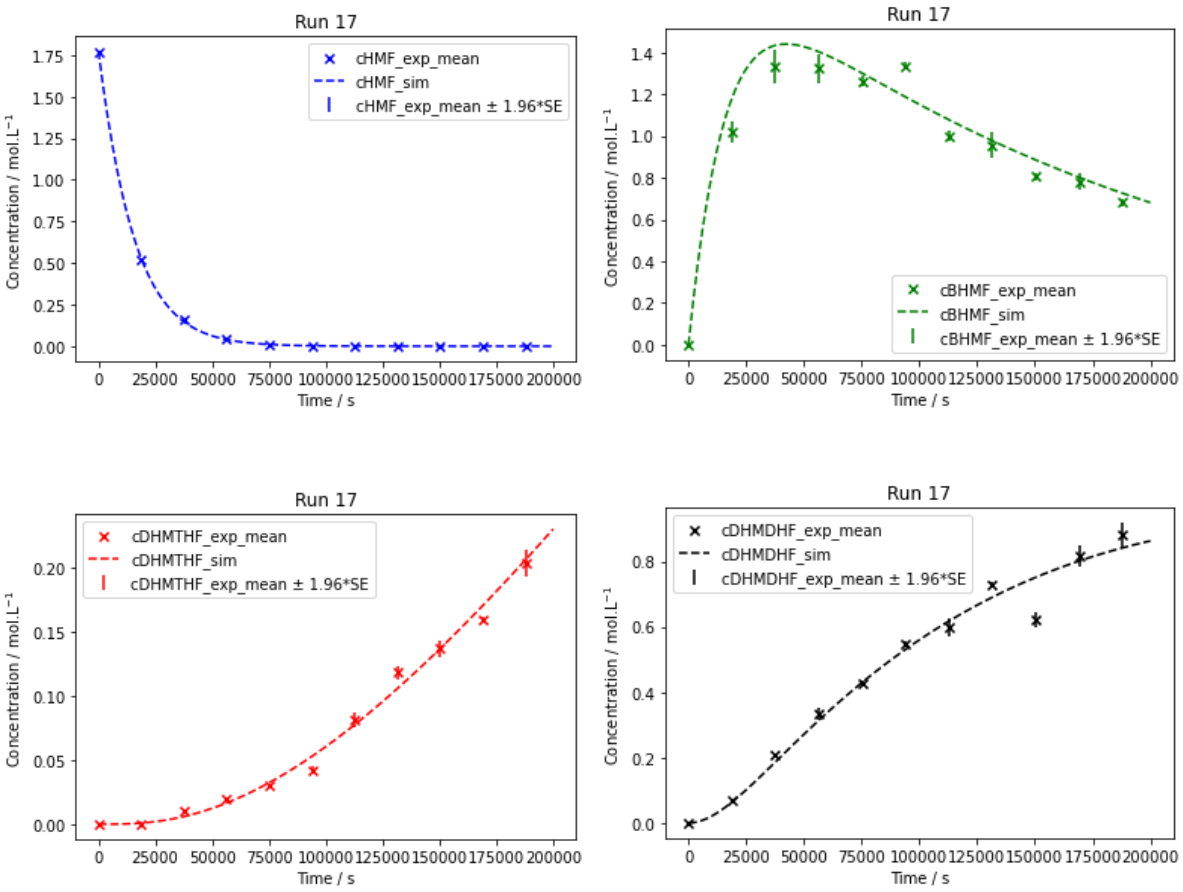

Figure 13. Fit of the model LHD1 to synthetic concentration with high error for Run 17H from Approach1H with error bars.

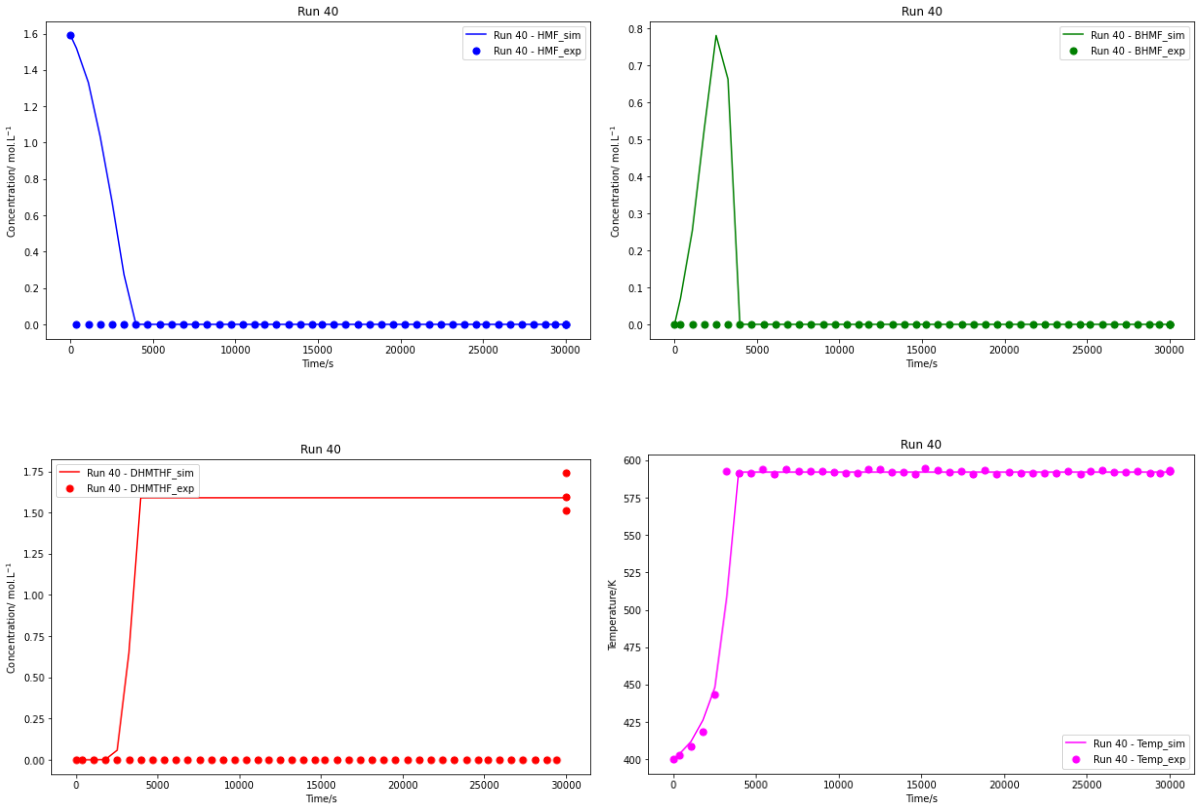

Figure 14. Fit of the model LHD1 to synthetic concentration with high error for Run 40H from Approach 6H.

This section evaluates the effect of the number of adiabatic synthetic runs on the sum of square of residuals (SSR). Each Approach has the same number of runs. One can find the Excel file Summary_LHD1_high_errors in repository Mendeley data (https://data.mendeley.com/datasets/v38n3wbsrt/1).

In order to compare the effect of the number of adiabatic synthetic runs on SSR, we divided this value by the number of synthetic points, n. Figures 15 and 16 show that SSR/n for the intermediate BHMF and DHMTHF are slightly higher than the other. One can observe that the use of Approach2H gives higher SSR/n values for the intermediate DHMTHF and for the reaction temperature. The kinetic modeling using Approach1H does not have SSR/n for temperature because synthetic runs were generated in isothermal conditions. Using Approach1H leads to slightly lower values of SSR/n for all species, globally. The SSR/n for all species for Approach1H and Approach3H to Approach6H is relatively similar. For SSR/n temperature, the use of Approach5H and Approach6H gives the lowest value.

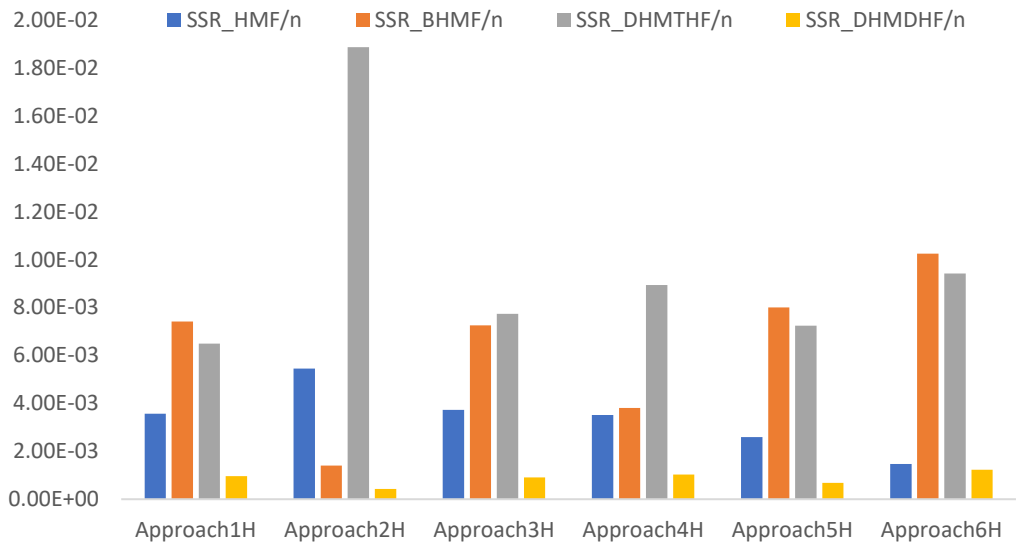

Figure 15. SSR/n from different Approach with all synthetic runs at high error values.

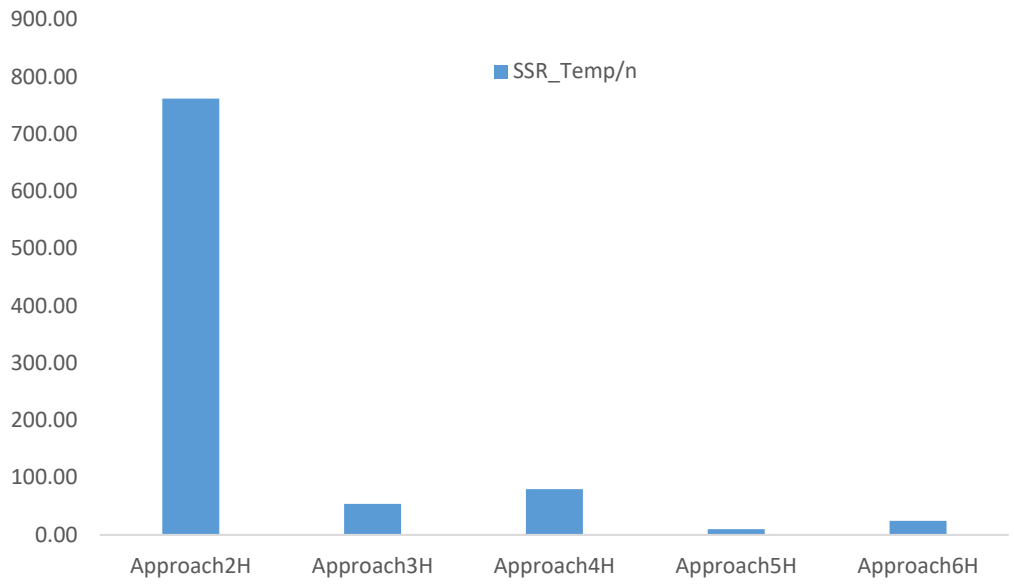

Figure 16. SSR/n from different Approach with all synthetic runs at high error values.

Figure 17 shows the effect of adiabatic synthetic runs at high errors. We did not include the HPD intervals for the sake of clarity.

From Figure 17, one can notice that the use of only adiabatic synthetic runs (Approach2H) gives the farthest estimated values from the true ones, and the use of only isothermal synthetic runs (Approach1H) gives the closer estimated values from the true ones. This observation is essentially verifiable for the estimation of the adsorption constants. This difference relies on the fact that the temperature response is the sum of the three reactions, thus making challenging the estimation.

Kinetic modeling with Approch5H and 6H, where more than 50% of runs were done in adiabatic conditions, allows a good estimation of the kinetic constants.

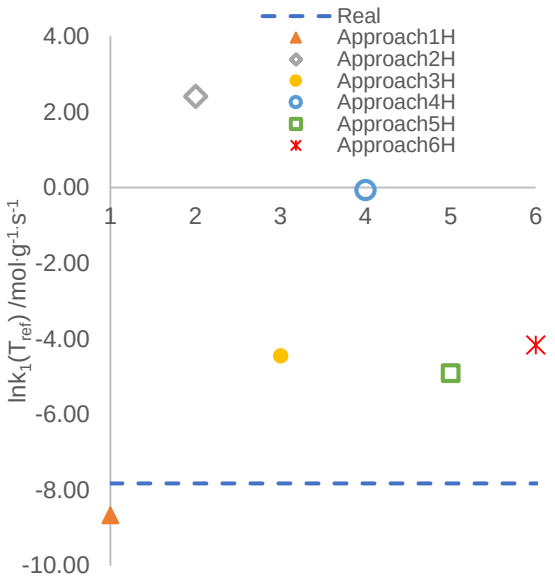
Real
Approach1H
Approach2H
Approach3H
Approach4H
Approach5H
Approach6H
4.00
2.00
0.00
-2.00
-4.00
-6.00
-8.00
-10.00
1
2
3
4
5
6
lnk1(Tref) /mol·g-1.s-1

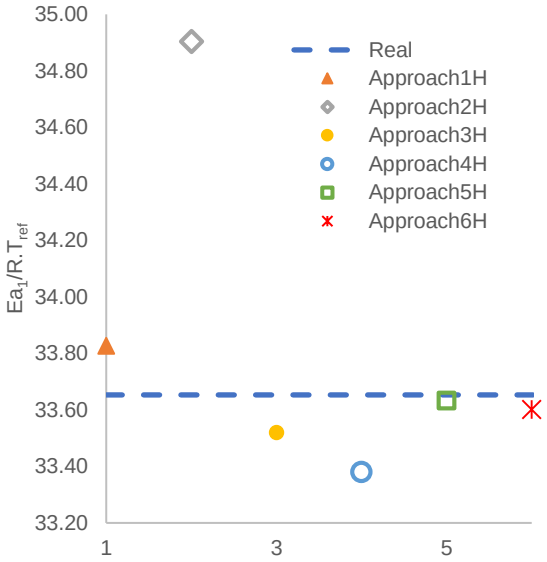
Real
Approach1H
Approach2H
Approach3H
Approach4H
Approach5H
Approach6H
35.00
34.80
34.60
34.40
34.20
34.00
33.80
33.60
33.40
33.20
1
3
5
Ea1/R.Tref

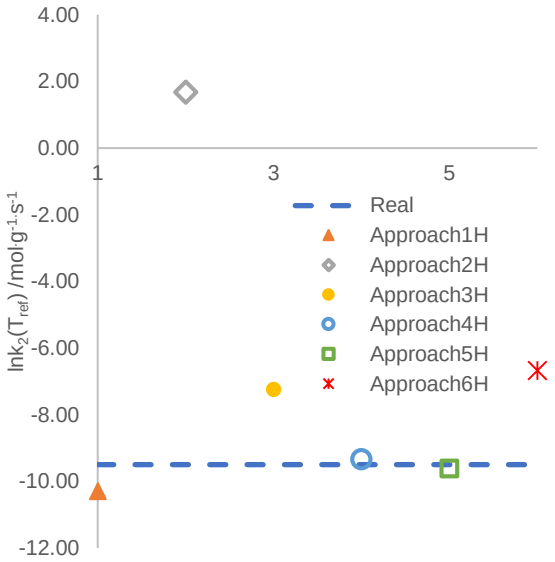
Real
Approach1H
Approach2H
Approach3H
Approach4H
Approach5H
Approach6H
4.00
2.00
0.00
-2.00
-4.00
-6.00
-8.00
-10.00
-12.00
1
3
5
lnk2(Tref) /mol·g-1.s-1

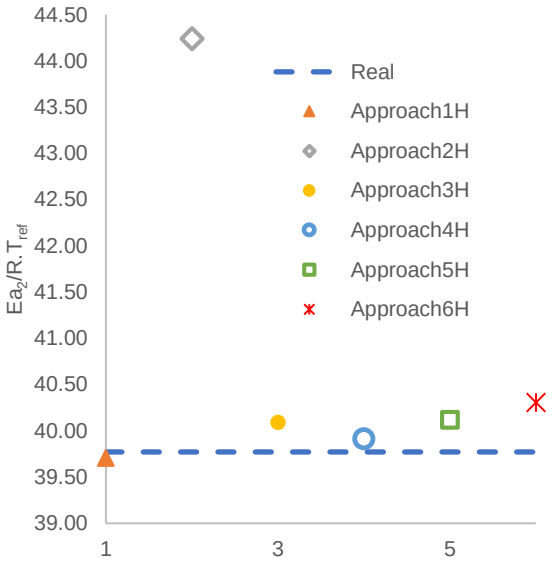
Real
Approach1H
Approach2H
Approach3H
Approach4H
Approach5H
Approach6H
44.50
44.00
43.50
43.00
42.50
42.00
41.50
41.00
40.50
40.00
39.50
39.00
1
3
5
Ea2/R.Tref

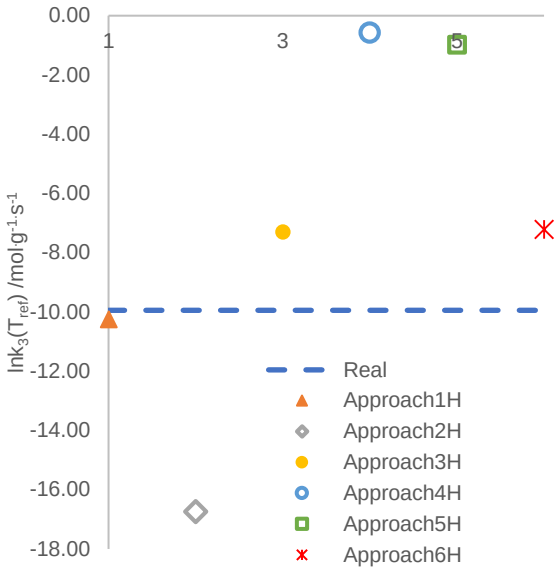
0.00
-2.00
-4.00
-6.00
-8.00
-10.00
-12.00
-14.00
-16.00
-18.00
1
3
lnk3(Tref) /mol·g-1·s-1
Real
Approach1H
Approach2H
Approach3H
Approach4H
Approach5H
Approach6H

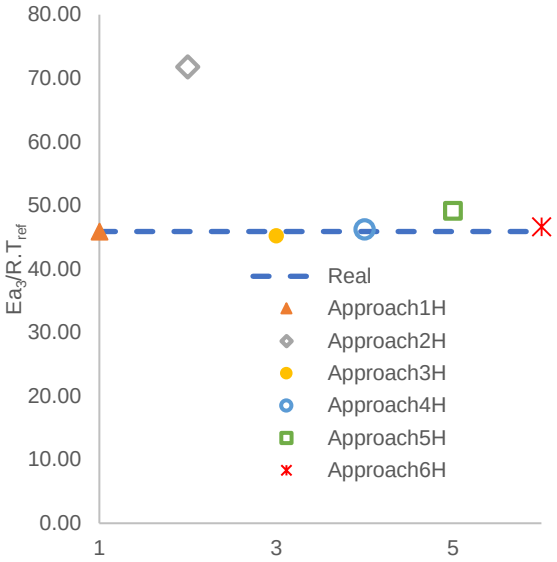
80.00
70.00
60.00
50.00
40.00
30.00
20.00
10.00
0.00
1
3
5
Ea3/R.Tref
Real
Approach1H
Approach2H
Approach3H
Approach4H
Approach5H
Approach6H

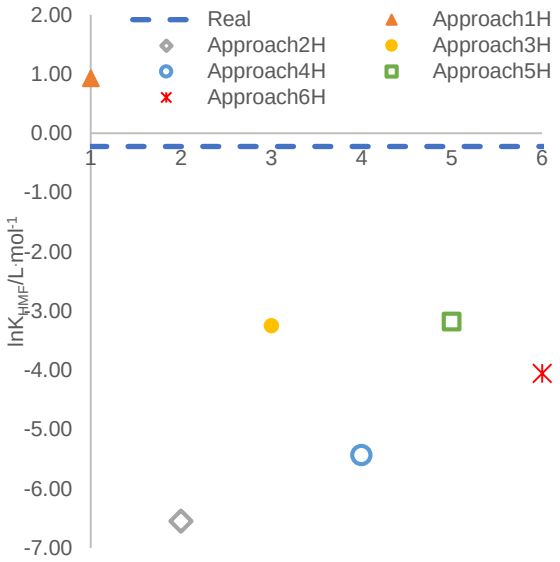
2.00
1.00
0.00
-1.00
-2.00
-3.00
-4.00
-5.00
-6.00
-7.00
1
2
3
4
5
6
lnKHMF/L·mol-1
Real
Approach1H
Approach2H
Approach3H
Approach4H
Approach5H
Approach6H

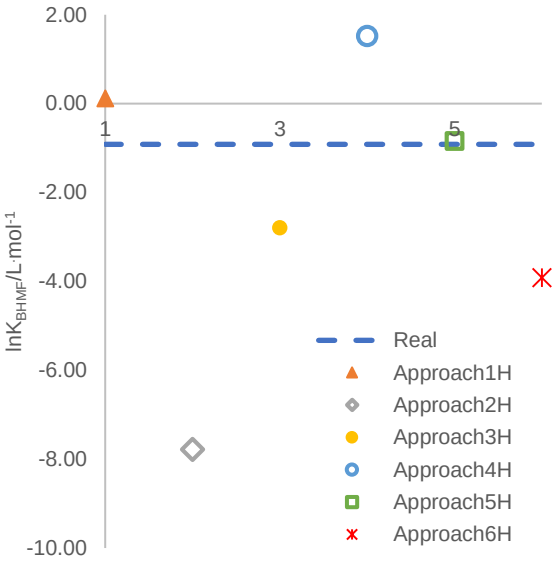
2.00
0.00
-2.00
-4.00
-6.00
-8.00
-10.00
1
3
5
lnKBHMF/L·mol-1
Real
Approach1H
Approach2H
Approach3H
Approach4H
Approach5H
Approach6H

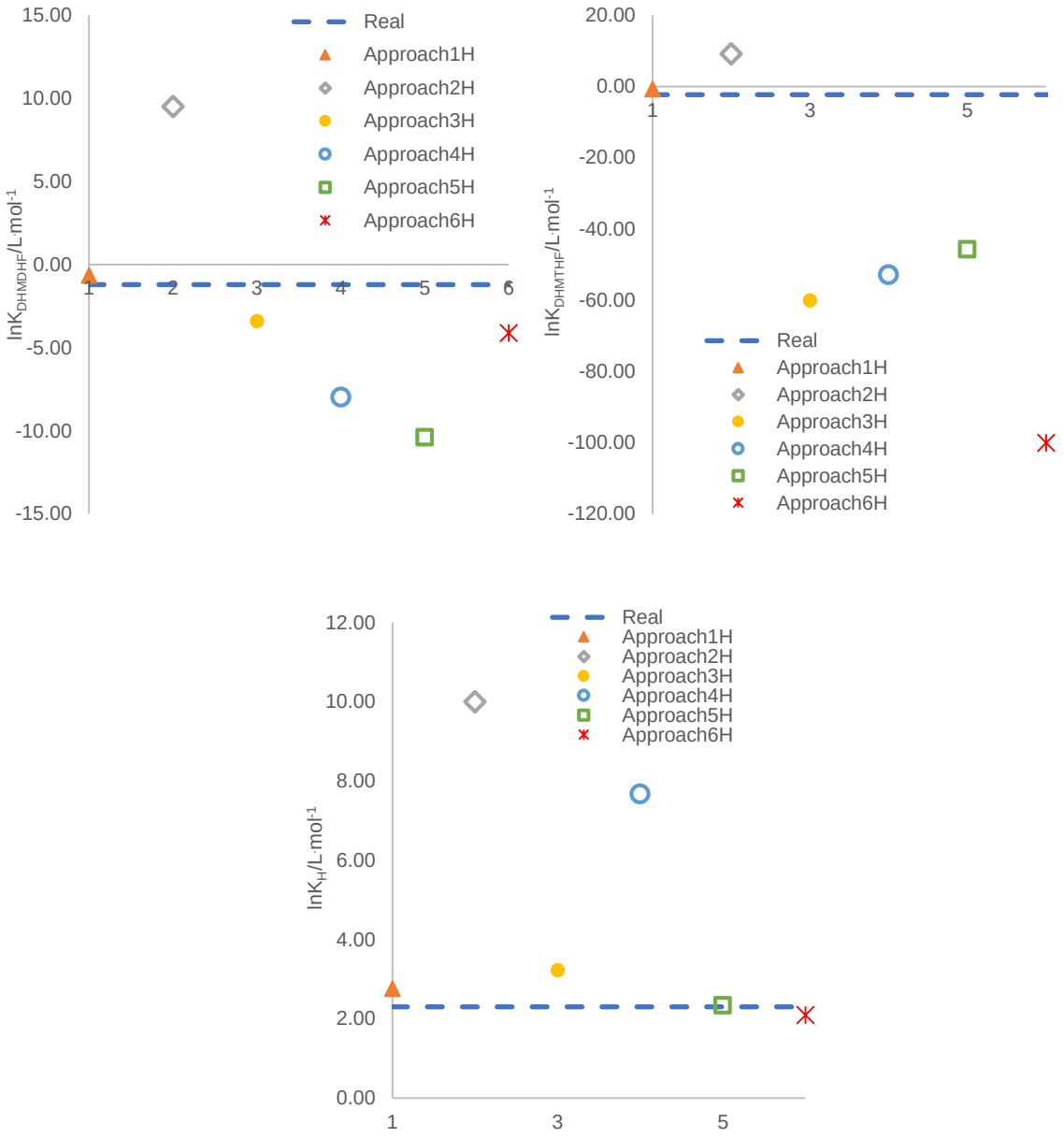

Figure 17. Effect of adiabatic synthetic runs with high errors for all Approaches towards hypothetical true kinetic constants (Real).

In general, kinetic models developed using high errors did not show strong correlations between the estimated parameters, and the parity plots show that the model can predict the concentration and temperature. The kinetic models are available in the repertory (https://data.mendeley.com/datasets/v38n3wbsrt/1).

5 Conclusions

This article deals with the impact of implementing adiabatic runs with isothermal runs for consecutive exothermic reaction steps, i.e., hydrogenation of 5-HMF. We created hypothetical true kinetic constants for Langmuir-Hinshelwood with the dissociation of hydrogen on the surface. Several synthetic runs were built from these hypothetical true kinetic constants, and two different error levels were added to the true synthetic concentration and temperature. The operating conditions were chosen as a kinetic modeler would have done, i.e., effect of initial temperature, concentration, pressure, catalyst loading, etc. These synthetic runs were done in a batch reactor and in isobaric mode. We created different approaches defined as a set of runs with different numbers of adiabatic and isothermal runs.

Estimating some kinetic constants, such as adsorption, is challenging. Hence, a global sensitivity analysis was done via the calculation of Sobol' indices in isothermal and adiabatic mode to know the most influential parameters (initial operating conditions and estimated kinetic constants) on ordinary differential equations (ODEs) from materials and energy balances. This analysis confirmed the difficulty of estimating the adsorption constants at the surface because their influence are low. In isothermal and adiabatic modes, this analysis showed that the kinetic constants for the first reaction step mainly influence the ODEs significantly.

By using 15 runs with low errors, i.e., standard deviation of 5% for concentration and 0.1K of temperature, we found that the ratio SSR/n for each observable, where n is the number of synthetic points, were similar for all approaches, except the one with only adiabatic runs. The ratio SSR/n obtained only for Approach using adiabatic runs were the higher ones. Such observation was also done for parameter estimation; the estimated kinetic constants were found to be far from the true ones by using solely adiabatic runs and were closed by using solely isothermal runs.

The use of 20 runs with high errors, i.e., a standard deviation of 13% for concentration and 1.0K of temperature, showed the same trend. It is impossible to correctly estimate kinetic constants solely with adiabatic runs for such reaction systems. Nevertheless, mixing adiabatic and isothermal runs gives similar estimated constants than the use of only isothermal runs.

Mixing adiabatic runs and isothermal runs for parameter estimation has two benefits. Firstly, it allows to decrease the analytical stage, and secondly it allows to get some models for product optimization, pinch analysis and thermal runaway assessment.

An extension of this work could be evaluating this approach in model selection. One of the main questions could be if different models, such as Eley-Rideal or non-competitive Langmuir-Hinshelwood, could be discriminated via adiabatic runs.

Notation

C_j	Concentration of species j
$C_{p,R}$	Standard heat capacity of reaction mixture
$C_{p,Cat}$	Standard heat capacity of the solid catalyst
E_{ai}	Activation energy of reaction step i
$He(T)$	Henry's constant
$[H_2]^*_{liq}$	Concentration of hydrogen at the gas-liquid interface
$\Delta H_{sol,H_2}$	Enthalpy of hydrogen solubilization
$\Delta H_{R,i}$	Reaction enthalpy of step i
$[j]_0$	Initial concentration of j
k_i	Rate constant of reaction i
$k_L.a$	Volumetric gas to liquid mass transfer coefficient for hydrogen
K_j	Adsoprtion constant of species j
m_R	Mass of reaction mixture
$m_{Catalyst}$	Mass of solid catalyst
OF	Objective function
$P_{H_2,reactor}$	Pressure of hydrogen in reactor
R	Universal gas constant
R_i	Reaction rate of step i
T	Temperature
T_{ref}	Reference temperature
V	Reaction volume

Greek letters

α	Number of events in response
β	Number of responses
$\lvert\nu\rvert$	Determinant of the covariance matrix of the responses
σ^2	Variance
ρ_{Liq}	Liquid density
μ_{Liq}	Kinematic viscosity
ω	Catalyst loading

Abbreviations

BHMF	2,5-Bishydroxymethylfuran
DHMDHF	2,5-Dihydroxymethyldihydrofuran
DHMTHF	2,5-Dihydroxymethyltetrahydrofuran
FTIR	Fourier-transform infrared spectroscopy
5-HMF	5-(Hydroxymethyl)furfural
GVL	γ-Valerolactone
HPD	Highest probability density in modeling estimation estimation
ODE	Ordinary differential equation
SSR	Sum of squared residuals
W	Water

Declaration of Competing Interest

The authors report no declarations of interest.

Associated Content

Supporting Information: Approaches for the modeling using synthetic runs with low errors; Modeling results using synthetic runs with low errors; Approaches for the modeling using synthetic runs with high errors; Modeling results using synthetic runs with high errors

Acknowledgements

This work was done in the framework of the PROMETEE project, standing for Processes to valoRize nOrman bioMass from renEwable energies: ciTizen sciencE and process safety. The author thanks Métropole Rouen Normandie for the funding.

References

(1) Pisano, R.; Capecchi, D. « La Théorie Analytique de La Chaleur » : Notes on Fourier et Lamé. *Bull. la Sabix* **2009**, No. 44, 87–93. https://doi.org/10.4000/sabix.683.

(2) Quílez, J. A Historical/Epistemological Account of the Foundation of the Key Ideas Supporting Chemical Equilibrium Theory. *Found. Chem.* **2019**, *21* (2), 221–252. https://doi.org/10.1007/s10698-018-9320-0.

(3) Habib Batis; Maurice Chastrette. Histoire de La Chimie Industrielle. *l'actualité Chim.* **2004**, *276*, 52–58.

(4) Arrhenius, S. Über Die Reaktionsgeschwindigkeit Bei Der Inversion von Rohrzucker Durch Säuren. *Zeitschrift für Phys. Chemie* **1889**, *4U* (1), 226–248. https://doi.org/10.1515/zpch-1889-0416.

(5) HinshelWood, C. N. The Kinetics of Chemical Change in Gaseous Systems. *J. Phys. Chem.* **1934**, *38* (6), 855–855. https://doi.org/10.1021/j150357a019.

(6) Villermaux, J. *Génie de La Réaction Chimique*; Tec & Doc Lavoisier, Ed.; Tec & Doc Lavoisier, 1993.

(7) Levenspiel, O. *Chemical Reaction Engineering. Essentials, Exercises and Examples*; John Wiley & Sons, 1998.

(8) Deem, M. C.; Cai, I.; Derasp, J. S.; Prieto, P. L.; Sato, Y.; Liu, J.; Kukor, A. J.; Hein, J. E. Best Practices for the Collection of Robust Time Course Reaction Profiles for Kinetic Studies. *ACS Catalysis*. American Chemical Society January 20, 2023, pp 1418–1430. https://doi.org/10.1021/acscatal.2c05045.

(9) Dreimann, J. M.; Kohls, E.; Warmeling, H. F. W.; Stein, M.; Guo, L. F.; Garland, M.; Dinh, T. N.; Vorholt, A. J. In Situ Infrared Spectroscopy as a Tool for Monitoring Molecular Catalyst for Hydroformylation in Continuous Processes. *ACS Catal.* **2019**, *9* (5), 4308–4319. https://doi.org/10.1021/acscatal.8b05066.

(10) Ni, L.; Qiu, W.; Jin, J.; Xu, Q.; Ye, S. Reaction Analysis and Process Optimization with Online Infrared Data Based on Kinetic Modeling and Partial Least Squares Quantitation. *Appl. Spectrosc.* **2022**, *76* (11), 1356–1366. https://doi.org/10.1177/00037028221123091.

(11) Musakka, N.; Salmi, T.; WärnÅ, J.; Ahlkvist, J.; Piironen, M. Modelling of Organic Liquid-Phase Decomposition Reactions through Gas-Phase Product Analysis: Model Systems and Peracetic Acid. *Chem. Eng. Sci.* **2006**, *61* (21), 6918–6928. https://doi.org/10.1016/j.ces.2006.07.033.

(12) Garcia-Hernandez, E. A.; Souza, C. R.; Vernières-Hassimi, L.; Leveneur, S. Kinetic Modeling Using Temperature as an Online Measurement: Application to the Hydrolysis of Acetic Anhydride, a Revisited Kinetic Model. *Thermochim. Acta* **2019**, *682*, 178409. https://doi.org/10.1016/j.tca.2019.178409.

(13) Snee, T. J.; Bassani, C.; Ligthart, J. A. M. Determination of the Thermokinetic Parameters of an Exothermic Reaction Using Isothermal, Adiabatic and Temperature-Programmed Calorimetry in Conjunction with Spectrophotometry. *J. Loss Prev. Process Ind.* **1993**, *6* (2), 87–94. https://doi.org/10.1016/0950-4230(93)90005-I.

(14) Hoffmann, W.; Kang, Y.; Mitchell, J. C.; Snowden, M. J. Kinetic Data by Nonisothermal Reaction Calorimetry: A Model-Assisted Calorimetric Evaluation. *Org. Process Res. Dev.* **2007**, *11* (1), 25–29. https://doi.org/10.1021/op060144j.

(15) Dobrosavljevic, I.; Schaer, E.; Commenge, J. M.; Falk, L. Intensification of a Highly Exothermic Chlorination Reaction Using a Combined Experimental and Simulation Approach for Fast Operating Conditions Prediction. *Chem. Eng. Process. Process Intensif.* **2016**, *105*, 46–63. https://doi.org/10.1016/j.cep.2016.04.007.

(16) Marco, E.; Cuartielles, S.; Pena, J. A.; Santamaria, J. Simulation of the Decomposition of Di-Cumyl Peroxide in an ARSST Unit. *Thermochim. Acta* **2000**, *362* (1–2), 49–58. https://doi.org/10.1016/S0040-6031(00)00587-6.

(17) Zogg, A.; Stoessel, F.; Fischer, U.; Hungerbühler, K. Isothermal Reaction Calorimetry as a Tool for Kinetic Analysis. *Thermochimica Acta*. Elsevier September 10, 2004, pp 1–17. https://doi.org/10.1016/j.tca.2004.01.015.

(18) Kossoy, A. Reaction Calorimetry: Main Types, Simple Theory, and Application for Kinetic Study—A Review. *Process Saf. Prog.* **2023**, *42* (3), 417–429. https://doi.org/10.1002/prs.12452.

(19) Vernières-Hassimi, L.; Dakkoune, A.; Abdelouahed, L.; Estel, L.; Leveneur, S. Zero-Order Versus Intrinsic Kinetics for the Determination of the Time to Maximum Rate under Adiabatic Conditions (TMRad): Application to the Decomposition of Hydrogen Peroxide. *Ind. Eng. Chem. Res.* **2017**, *56* (45), 13040–13049. https://doi.org/10.1021/acs.iecr.7b01291.

(20) Stoessel, F. *Thermal Safety of Chemical Processes: Risk Assessment and Process Design*; Wiley-VCH, 2008. https://doi.org/10.1002/9783527621606.

(21) Salcedo, W. N. V.; Mignot, M.; Renou, B.; Leveneur, S. Assessment of Kinetic Models for the Production of γ-Valerolactone Developed in Isothermal, Adiabatic and Isoperibolic Conditions. *Fuel* **2023**, *350*, 128792. https://doi.org/10.1016/j.fuel.2023.128792.

(22) Andreozzi, R.; Canterino, M.; Caprio, V.; Di Somma, I.; Sanchirico, R. Batch Salicylic Acid Nitration by Nitric Acid/Acetic Acid Mixture under Isothermal, Isoperibolic and Adiabatic Conditions. *J. Hazard. Mater.* **2006**, *138* (3), 452–458. https://doi.org/10.1016/j.jhazmat.2006.05.104.

(23) Leonhardt, J.; Hugo, P. Comparison of Thermokinetic Data Obtained by Isothermal, Isoperibolic, Adiabatic and Temperature Programmed Measurements. *J. Therm. Anal.* **1997**, *49* (3), 1535–1551. https://doi.org/10.1007/bf01983714.

(24) De Oliveira, L. P.; Hudebine, D.; Guillaume, D.; Verstraete, J. J. A Review of Kinetic

Modeling Methodologies for Complex Processes. *Oil Gas Sci. Technol.* **2016**, *71* (3), 45. https://doi.org/10.2516/ogst/2016011.

(25) Xing, Y.; Dong, Y.; Zhou, W.; Du, J.; Meng, Q. Optimization-Based Simultaneous Modelling of Stoichiometries and Kinetics in Complex Organic Reaction System. *Chem. Eng. Sci.* **2023**, *276*, 118758. https://doi.org/10.1016/j.ces.2023.118758.

(26) Leveneur, S. Kinetic Modelling: Regression and Validation Stages, a Compulsory Tandem for Kinetic Model Assessment. *Can. J. Chem. Eng.* **2023**, *101* (12), 7078–7101. https://doi.org/10.1002/cjce.24956.

(27) Wang, H.; Zhu, C.; Li, D.; Liu, Q.; Tan, J.; Wang, C.; Cai, C.; Ma, L. Recent Advances in Catalytic Conversion of Biomass to 5-Hydroxymethylfurfural and 2, 5-Dimethylfuran. *Renewable and Sustainable Energy Reviews*. Pergamon April 1, 2019, pp 227–247. https://doi.org/10.1016/j.rser.2018.12.010.

(28) Hu, L.; Lin, L.; Wu, Z.; Zhou, S.; Liu, S. Recent Advances in Catalytic Transformation of Biomass-Derived 5-Hydroxymethylfurfural into the Innovative Fuels and Chemicals. *Renewable and Sustainable Energy Reviews*. Pergamon July 1, 2017, pp 230–257. https://doi.org/10.1016/j.rser.2017.02.042.

(29) Chen, S.; Wojcieszak, R.; Dumeignil, F.; Marceau, E.; Royer, S. How Catalysts and Experimental Conditions Determine the Selective Hydroconversion of Furfural and 5-Hydroxymethylfurfural. *Chemical Reviews*. American Chemical Society November 28, 2018, pp 11023–11117. https://doi.org/10.1021/acs.chemrev.8b00134.

(30) Zhao, W.; Wu, W.; Li, H.; Fang, C.; Yang, T.; Wang, Z.; He, C.; Yang, S. Quantitative Synthesis of 2,5-Bis(Hydroxymethyl)Furan from Biomass-Derived 5-Hydroxymethylfurfural and Sugars over Reusable Solid Catalysts at Low Temperatures. *Fuel* **2018**, *217*, 365–369. https://doi.org/10.1016/j.fuel.2017.12.069.

(31) Wiesfeld, J. J.; Kim, M.; Nakajima, K.; Hensen, E. J. M. Selective Hydrogenation of 5-

Hydroxymethylfurfural and Its Acetal with 1,3-Propanediol to 2,5-Bis(Hydroxymethyl)Furan Using Supported Rhenium-Promoted Nickel Catalysts in Water. *Green Chem.* **2020**, *22* (4), 1229–1238. https://doi.org/10.1039/c9gc03856f.

(32) Gyngazova, M. S.; Negahdar, L.; Blumenthal, L. C.; Palkovits, R. Experimental and Kinetic Analysis of the Liquid Phase Hydrodeoxygenation of 5-Hydroxymethylfurfural to 2,5-Dimethylfuran over Carbon-Supported Nickel Catalysts. *Chem. Eng. Sci.* **2017**, *173*, 455–464. https://doi.org/10.1016/j.ces.2017.07.045.

(33) Li, S.; Dong, M.; Yang, J.; Cheng, X.; Shen, X.; Liu, S.; Wang, Z. Q.; Gong, X. Q.; Liu, H.; Han, B. Selective Hydrogenation of 5-(Hydroxymethyl)Furfural to 5-Methylfurfural over Single Atomic Metals Anchored on Nb2O5. *Nat. Commun.* **2021**, *12* (1), 1–9. https://doi.org/10.1038/s41467-020-20878-7.

(34) Zhao, W.; Wang, F.; Zhao, K.; Liu, X.; Zhu, X.; Yan, L.; Yin, Y.; Xu, Q.; Yin, D. Recent Advances in the Catalytic Production of Bio-Based Diol 2,5-Bis(Hydroxymethyl)Furan. *Carbon Resources Conversion*. Elsevier June 1, 2023, pp 116–131. https://doi.org/10.1016/j.crcon.2023.01.001.

(35) Deussen, P.; Galvanin, F. A Model-Based Experimental Design Approach to Assess the Identifiability of Kinetic Models of Hydroxymethylfurfural Hydrogenation in Batch Reaction Systems. *Chem. Eng. Res. Des.* **2022**, *178*, 609–622. https://doi.org/10.1016/j.cherd.2021.12.028.

(36) Gawade, A. B.; Tiwari, M. S.; Yadav, G. D. Biobased Green Process: Selective Hydrogenation of 5-Hydroxymethylfurfural to 2,5-Dimethyl Furan under Mild Conditions Using Pd-Cs2.5H0.5PW12O40/K-10 Clay. *ACS Sustain. Chem. Eng.* **2016**, *4* (8), 4113–4123. https://doi.org/10.1021/acssuschemeng.6b00426.

(37) Jain, A. B.; Vaidya, P. D. Kinetics of Catalytic Hydrogenation of 5-Hydroxymethylfurfural to 2,5-Bis-Hydroxymethylfuran in Aqueous Solution over Ru/C. *Int. J. Chem. Kinet.* **2016**, *48* (6), 318–328. https://doi.org/10.1002/kin.20992.

(38) Capecci, S.; Wang, Y.; Casson Moreno, V.; Held, C.; Leveneur, S. Solvent Effect on the Kinetics of the Hydrogenation of N-Butyl Levulinate to γ-Valerolactone. *Chem. Eng. Sci.* **2021**, *231*, 116315. https://doi.org/10.1016/j.ces.2020.116315.

(39) Buzzi-Ferraris, G. Planning of Experiments and Kinetic Analysis. *Catal. Today* **1999**, *52* (2–3), 125–132. https://doi.org/10.1016/S0920-5861(99)00070-X.

(40) Vasiliu, M.; Jones, A. J.; Guynn, K.; Dixon, D. A. Prediction of the Thermodynamic Properties of Key Products and Intermediates from Biomass. II. *J. Phys. Chem. C* **2012**, *116* (39), 20738–20754. https://doi.org/10.1021/jp306596d.

(41) Wang, Y.; Cipolletta, M.; Vernières-Hassimi, L.; Casson-Moreno, V.; Leveneur, S. Application of the Concept of Linear Free Energy Relationships to the Hydrogenation of Levulinic Acid and Its Corresponding Esters. *Chem. Eng. J.* **2019**, *374*, 822–831. https://doi.org/10.1016/j.cej.2019.05.218.

(42) Ariba, H.; Wang, Y.; Devouge-Boyer, C.; Stateva, R. P.; Leveneur, S. Physicochemical Properties for the Reaction Systems: Levulinic Acid, Its Esters, and γ-Valerolactone. *J. Chem. Eng. Data* **2020**, *65* (6), 3008–3020. https://doi.org/10.1021/acs.jced.9b00965.

(43) Lu, X.; Wang, Y.; Estel, L.; Kumar, N.; Grénman, H.; Leveneur, S. Evolution of Specific Heat Capacity with Temperature for Typical Supports Used for Heterogeneous Catalysts. *Processes* **2020**, *8* (8), 911. https://doi.org/10.3390/PR8080911.

(44) Caracotsios, M.; Stewart, W. E. Sensitivity Analysis of Initial Value Problems with Mixed Odes and Algebraic Equations. *Comput. Chem. Eng.* **1985**, *9* (4), 359–365. https://doi.org/10.1016/0098-1354(85)85014-6.

(45) Stewart, W. E.; Caracotsios, M. *Computer-Aided Modeling of Reactive Systems*, First.; Wiley & Sons, Ed.; New Jersey, 2008. https://doi.org/10.1002/9780470282038.

(46) Garcia-Hernandez, E. A.; Elmoukrie, M. E.; Leveneur, S.; Gourich, B.; Vernieres-Hassimi, L. Global Sensitivity Analysis to Identify Influential Model Input on Thermal

Risk Parameters: To Cottonseed Oil Epoxidation. *J. Loss Prev. Process Ind.* **2022**, *77*, 104795. https://doi.org/10.1016/j.jlp.2022.104795.

(47) Zhang, X. Y.; Trame, M. N.; Lesko, L. J.; Schmidt, S. Sobol Sensitivity Analysis: A Tool to Guide the Development and Evaluation of Systems Pharmacology Models. *CPT: Pharmacometrics and Systems Pharmacology*. John Wiley & Sons, Ltd February 1, 2015, pp 69–79. https://doi.org/10.1002/psp4.6.

(48) Herman, J.; Usher, W. SALib: An Open-Source Python Library for Sensitivity Analysis. *J. Open Source Softw.* **2017**, *2* (9), 97. https://doi.org/10.21105/joss.00097.

(49) Stewart, W. E.; Caracotsios, M.; Sørensen, J. P. Parameter Estimation from Multiresponse Data. *AIChE Journal*. John Wiley & Sons, Ltd May 1, 1992, pp 641–650. https://doi.org/10.1002/aic.690380502.

(50) Kopyscinski, J.; Choi, J.; Hill, J. M. Comprehensive Kinetic Study for Pyridine Hydrodenitrogenation on (Ni)WP/SiO2 Catalysts. *Appl. Catal. A Gen.* **2012**, *445–446*, 50–60. https://doi.org/10.1016/j.apcata.2012.08.027.

(51) Box, G. E. P.; Draper, N. R. The Bayesian Estimation of Common Parameters from Several Responses. *Biometrika* **1965**, *52* (3–4), 355–365. https://doi.org/10.1093/biomet/52.3-4.355.

(52) van Boekel, M. A. J. S. On the Pros and Cons of Bayesian Kinetic Modeling in Food Science. *Trends in Food Science and Technology*. Elsevier May 1, 2020, pp 181–193. https://doi.org/10.1016/j.tifs.2020.02.027.

(53) Toch, K.; Thybaut, J. W.; Marin, G. B. A Systematic Methodology for Kinetic Modeling of Chemical Reactions Applied to N-Hexane Hydroisomerization. *AIChE J.* **2015**, *61* (3), 880–892. https://doi.org/10.1002/aic.14680.